Supplement of "Simulating liquid water distribution at the pore scale in snow: water retention curves and effective transport properties"

Lisa Bouvet[1,2], Nicolas Allet[1,2], Neige Calonne[1], Frédéric Flin[1], and Christian Geindreau[2]

[1]Univ. Grenoble Alpes, Université de Toulouse, Météo-France, CNRS, CNRM, Centre d'Études de la Neige, Grenoble, France

[2]Université Grenoble Alpes, CNRS, Grenoble INP, 3SR, Grenoble, France

Description

The 34 images of the dataset used in this study are presented hereafter.

A first table, p. 2, lists all the images of the dataset, together with their snow type (Fierz et al., 2009), their provenance and/or main preparation procedure, and a reference where more information on the image can be obtained.

A second table, p. 3, provides the side length (in number of voxels) and pixel size (in µm) of the cubic volumes, together with the main properties of the sample: density ρ (kg m^{-3}), specific surface area SSA (m^2 kg^{-1}), equivalent grain diameter d (mm), mean value of the mean curvature $\overline{\mathrm{MC}}$ (mm^{-1}) and interquartile range of the mean curvature $\mathrm{IQR}_{\mathrm{MC}}$ (mm^{-1}).

From p. 4 to 37, each image is presented in details, with a property table, downward and upward views, and a mean curvature histogram.

Table S1. List of the 34 images used in this study.

Image	Snow type	Comment	Main reference
fr	PP	Sampled at Col de Porte (1325 m altitude, Chartreuse range, France), 14 February 2002.	Calonne et al. (2011)
I01	PP	Sampled at Col de Porte (1325 m altitude, Chartreuse range, France), 15 h after the snowfall.	Flin et al. (2004)
I03	PP	62 h after the snowfall, under isothermal conditions at –2°C.	Flin et al. (2004)
I04	PP	81 h after the snowfall, under isothermal conditions at –2°C.	Flin et al. (2004)
I08	DF	297 h after the snowfall, under isothermal conditions at –2°C.	Flin et al. (2004)
I15	RG	806 h after the snowfall, under isothermal conditions at –2°C.	Flin et al. (2004)
I19	RG	1381 h after the snowfall, under isothermal conditions at –2°C.	Flin et al. (2004)
I21	RG	1694 h after the snowfall, under isothermal conditions at –2°C.	Flin et al. (2004)
I23	RG	2026 h after the snowfall, under isothermal conditions at –2°C.	Flin et al. (2004)
P03	PP	Girose glacier (3200 m altitude, Ecrins range, France), 20 cm depth, 17 March 2009.	Flin et al. (2011)
P04	DF	Girose glacier (3200 m altitude, Ecrins range, France), 40 cm depth, 17 March 2009.	Flin et al. (2011)
P06	RG	Girose glacier (3200 m altitude, Ecrins range, France), 60 cm depth, 17 March 2009.	Flin et al. (2011)
P07	RG	Girose glacier (3200 m altitude, Ecrins range, France), 70 cm depth, 17 March 2009.	Flin et al. (2011)
P08	RG	Girose glacier (3200 m altitude, Ecrins range, France), 100 cm depth, 17 March 2009.	Flin et al. (2011)
P09	RG	Girose glacier (3200 m altitude, Ecrins range, France), 120 cm depth, 17 March 2009.	Flin et al. (2011)
P10	RG	Girose glacier (3200 m altitude, Ecrins range, France), 165 cm depth, 17 March 2009.	Flin et al. (2011)
P11	RG	Girose glacier (3200 m altitude, Ecrins range, France), 65 cm depth, 1 March 2009.	Flin et al. (2011)
P14	RG	Girose glacier (3200 m altitude, Ecrins range, France), 80 cm depth, 1 March 2009.	Flin et al. (2011)
P15	RG	Girose glacier (3200 m altitude, Ecrins range, France), 170 cm depth, 1 March 2009.	Flin et al. (2011)
NH0	RG	Sieved snow, followed by isothermal conditions.	Flin et al. (2011)
NH1	MF	Grain coarsening of water-saturated snow and drainage after 1h.	Flin et al. (2011)
NH12	MF	Grain coarsening of water-saturated snow and drainage after 6h.	Flin et al. (2011)
NH2	MF	Grain coarsening of water-saturated snow and drainage after 24h.	Flin et al. (2011)
NH5	MF	Grain coarsening of water-saturated snow and drainage after 142h.	Flin et al. (2011)
cham	MF	Grain coarsening of water-saturated snow and drainage.	Coléou et al. (2001)
E2b	FC	3 weeks under a TG = 16 K m-1 , T mean = -3°C, sampled in the middle of the layer.	Flin and Brzoska (2008)
0A	RG	Sieved snow, followed by isothermal conditions.	Calonne et al. (2014)
1A	RG	3 days under a TG = 43 K m-1, T mean = -4°C, sampled in the middle of the layer.	Calonne et al. (2014)
2A	FC	6 days under a TG = 43 K m-1, T mean = -4°C, sampled in the middle of the layer.	Calonne et al. (2014)
3A	DH	9 days under a TG = 43 K m-1, T mean = -4°C, sampled in the middle of the layer.	Calonne et al. (2014)
4A	DH	13 days under a TG = 43 K m-1 , T mean = -4°C, sampled in the middle of the layer.	Calonne et al. (2014)
5A	DH	17 days under a TG = 43 K m-1 , T mean = -4°C, sampled in the middle of the layer.	Calonne et al. (2014)
7A	DH	21 days under a TG = 43 K m-1 , T mean = -4°C, sampled in the middle of the layer.	Calonne et al. (2014)
grad3	DH	8 days under a TG = 100 K m-1 , T mean = -5°C.	Coléou et al. (2001)

Table S2. Properties of the 34 images used in this study.

Image	Snow type	Image size (voxel)	Pixel size (μm)	ρ (kg m^{-3})	SSA (m^2 kg^{-1})	d (mm)	$\overline{\mathrm{MC}}$ (mm^{-1})	$\mathrm{IQR}_{\mathrm{MC}}$ (mm^{-1})
fr	PP	1192	4.910	124.88	55.30	0.1183	8.07	21.83
I01	PP	512	4.910	102.90	55.79	0.1173	8.19	17.45
I03	PP	600	4.910	123.31	41.37	0.1581	6.08	13.18
I04	PP	600	4.910	113.44	42.48	0.1540	6.49	13.03
I08	DF	512	4.910	147.71	29.32	0.2232	5.27	8.80
I15	RG	600	4.910	172.74	23.32	0.2805	4.10	6.54
I19	RG	600	4.910	192.47	19.90	0.3288	3.47	5.80
I21	RG	600	4.910	198.64	19.23	0.3402	3.28	5.58
I23	RG	512	4.910	256.28	17.24	0.3804	2.54	4.75
P03	PP	512	8.480	134.60	50.91	0.1285	13.16	14.99
P04	DF	512	8.588	157.58	25.36	0.2580	5.10	7.08
P06	RG	512	6.158	354.51	21.59	0.3031	3.30	6.45
P07	RG	512	8.609	280.07	17.15	0.3816	3.01	5.29
P08	RG	512	8.552	378.96	14.57	0.4490	1.85	4.84
P09	RG	512	6.158	396.13	12.29	0.5325	1.61	5.15
P10	RG	512	6.103	396.07	10.46	0.6253	1.25	4.78
P11	RG	512	8.588	413.71	20.76	0.3151	3.13	7.18
P14	RG	600	6.154	359.84	18.13	0.3608	2.35	6.86
P15	RG	512	6.158	315.50	16.09	0.4067	2.65	5.65
NH0	RG	651	8.609	430.59	17.34	0.3773	2.37	6.61
NH1	MF	651	8.609	544.08	6.99	0.9363	-0.05	8.10
NH12	MF	651	8.590	512.89	7.69	0.8514	0.14	6.82
NH2	MF	651	8.590	502.60	6.18	1.0584	0.31	5.15
NH5	MF	1000	9.460	472.83	3.78	1.7302	0.35	3.08
cham	MF	542	10.000	522.31	8.49	0.7702	0.13	6.90
E2b	FC	1200	4.910	262.74	15.43	0.4240	1.99	7.64
0A	RG	700	8.392	314.83	27.68	0.2367	4.87	9.38
1A	RG	700	8.395	275.04	23.37	0.2800	4.67	9.17
2A	FC	700	8.373	282.70	20.75	0.3154	3.53	9.03
3A	DH	700	8.400	274.79	18.18	0.3600	2.65	8.52
4A	DH	700	8.397	315.31	15.19	0.4309	1.34	7.61
5A	DH	1000	9.655	286.12	14.89	0.4395	1.65	7.75
7A	DH	950	9.672	309.95	13.42	0.4882	1.05	7.87
grad3	DH	600	10.000	369.20	21.84	0.2996	0.76	11.32

Image fr

Table S3.

Snow type	Image size (voxel)	Pixel size (µm)	ρ (kg m^{-3})	SSA (m^2 kg^{-1})	d (mm)	$\overline{\mathrm{MC}}$ (mm^{-1})	IQR$_{\mathrm{MC}}$ (mm^{-1})
PP	1192	4.910	124.88	55.30	0.1183	8.07	21.83

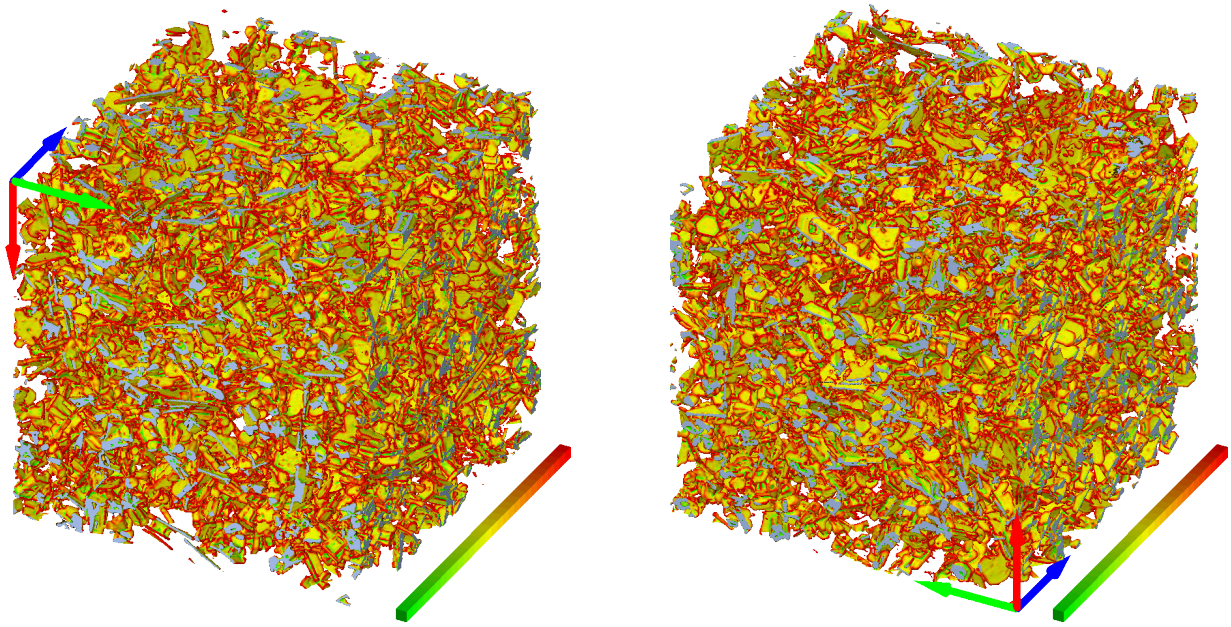

Figure S1. Downward (left) and upward (right) views of the whole image volume, where the mean local curvature is represented in each point of the surface. Concave surfaces are shown in green, convex surfaces in red, and flat surfaces in yellow (see colorbars from -30 to +30 mm^{-1}). The side of each viewing cube amounts to 5.85 mm. The blue, green, and red arrows, correspond to the x, y, and z coordinate axes, respectively.

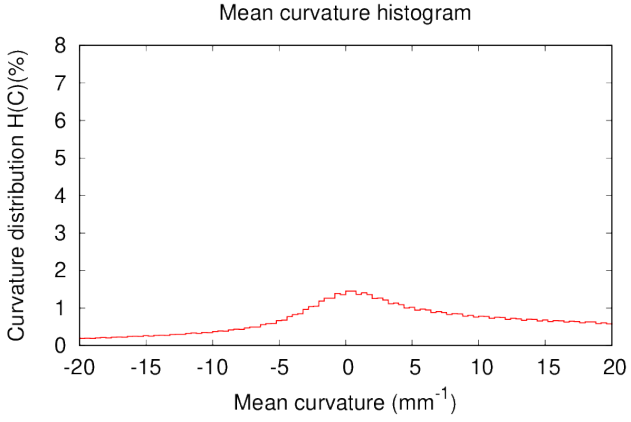

Figure S2. Mean curvature distribution on the whole image, from -20 to +20 mm^{-1}. Each bin is 0.4 mm^{-1} wide.

Image I01

Table S4.

Snow type	Image size (voxel)	Pixel size (µm)	ρ (kg m^{-3})	SSA (m^2 kg^{-1})	d (mm)	$\overline{\mathrm{MC}}$ (mm^{-1})	IQR$_{\mathrm{MC}}$ (mm^{-1})
PP	512	4.910	102.90	55.79	0.1173	8.19	17.45

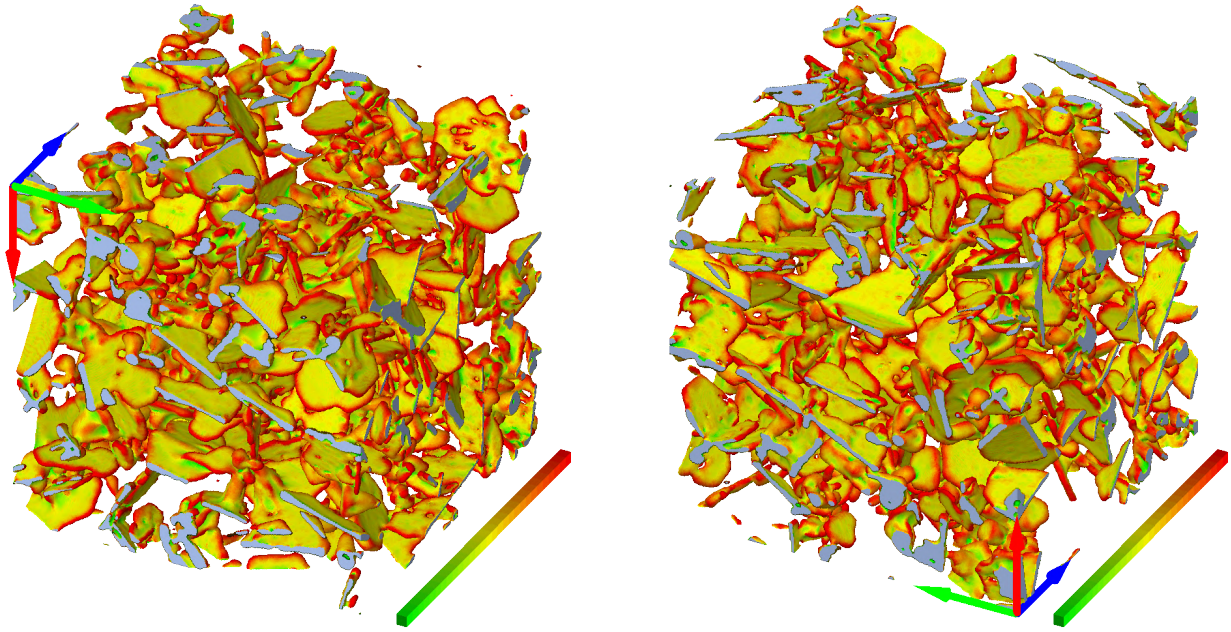

Figure S3. Downward (left) and upward (right) views of the whole image volume, where the mean local curvature is represented in each point of the surface. Concave surfaces are shown in green, convex surfaces in red, and flat surfaces in yellow (see colorbars from -30 to +30 mm^{-1}). The side of each viewing cube amounts to 2.51 mm. The blue, green, and red arrows, correspond to the x, y, and z coordinate axes, respectively.

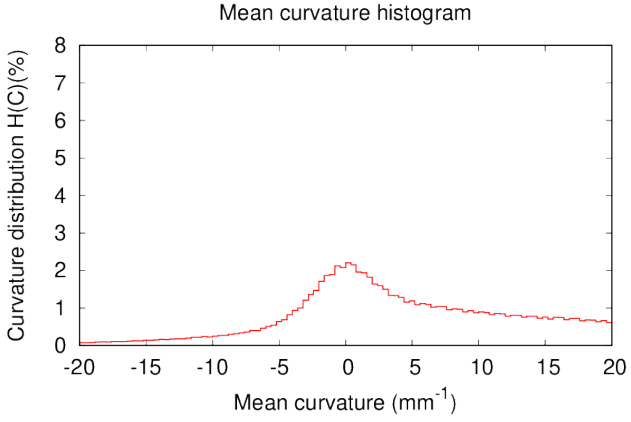

Figure S4. Mean curvature distribution on the whole image, from -20 to +20 mm^{-1}. Each bin is 0.4 mm^{-1} wide.

Image I03

Table S5.

Snow type	Image size (voxel)	Pixel size (µm)	ρ (kg m^{-3})	SSA (m^2 kg^{-1})	d (mm)	$\overline{\mathrm{MC}}$ (mm^{-1})	IQR$_{\mathrm{MC}}$ (mm^{-1})
PP	600	4.910	123.31	41.37	0.1581	6.08	13.18

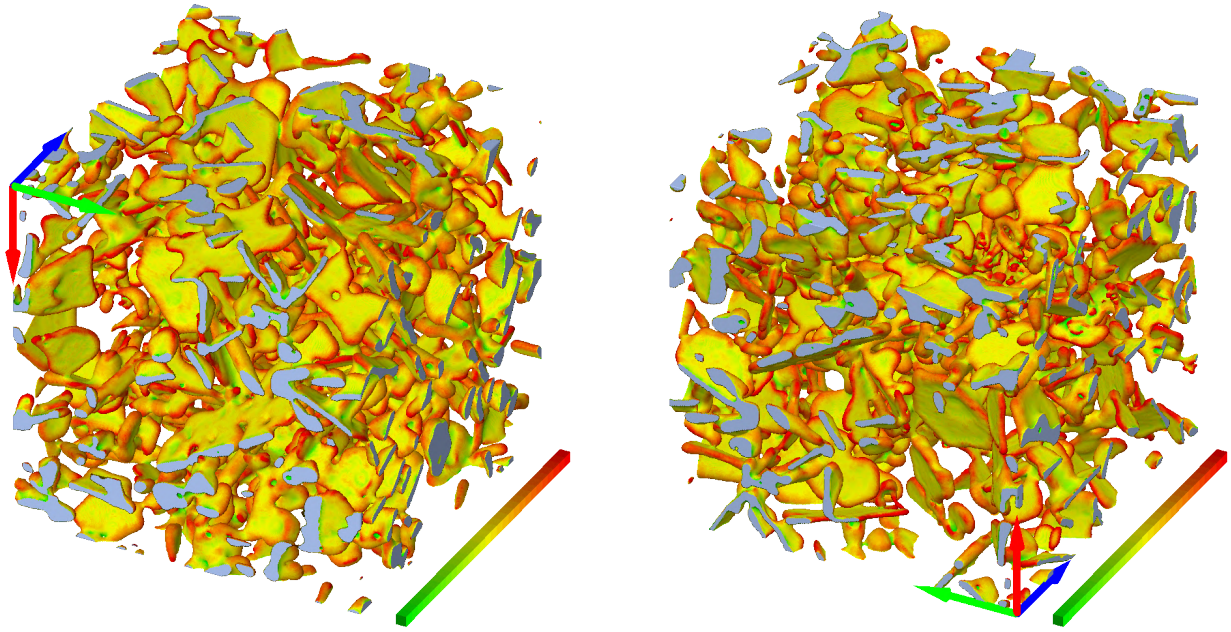

Figure S5. Downward (left) and upward (right) views of the whole image volume, where the mean local curvature is represented in each point of the surface. Concave surfaces are shown in green, convex surfaces in red, and flat surfaces in yellow (see colorbars from -30 to +30 mm^{-1}). The side of each viewing cube amounts to 2.95 mm. The blue, green, and red arrows, correspond to the x, y, and z coordinate axes, respectively.

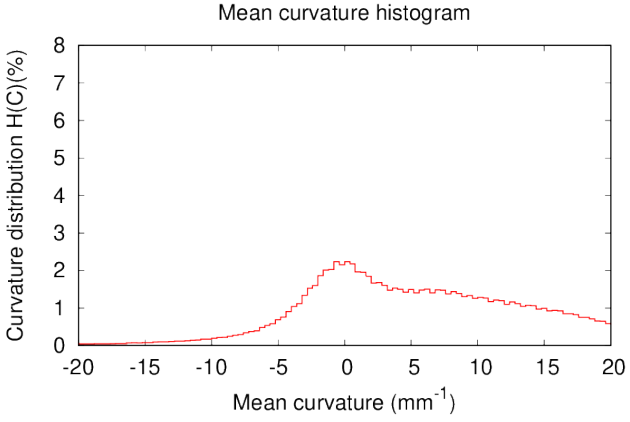

Figure S6. Mean curvature distribution on the whole image, from -20 to +20 mm^{-1}. Each bin is 0.4 mm^{-1} wide.

Image I04

Table S6.

Snow type	Image size (voxel)	Pixel size (µm)	ρ (kg m^{-3})	SSA (m^2 kg^{-1})	d (mm)	$\overline{\mathrm{MC}}$ (mm^{-1})	IQR$_{\mathrm{MC}}$ (mm^{-1})
PP	600	4.910	113.44	42.48	0.1540	6.49	13.03

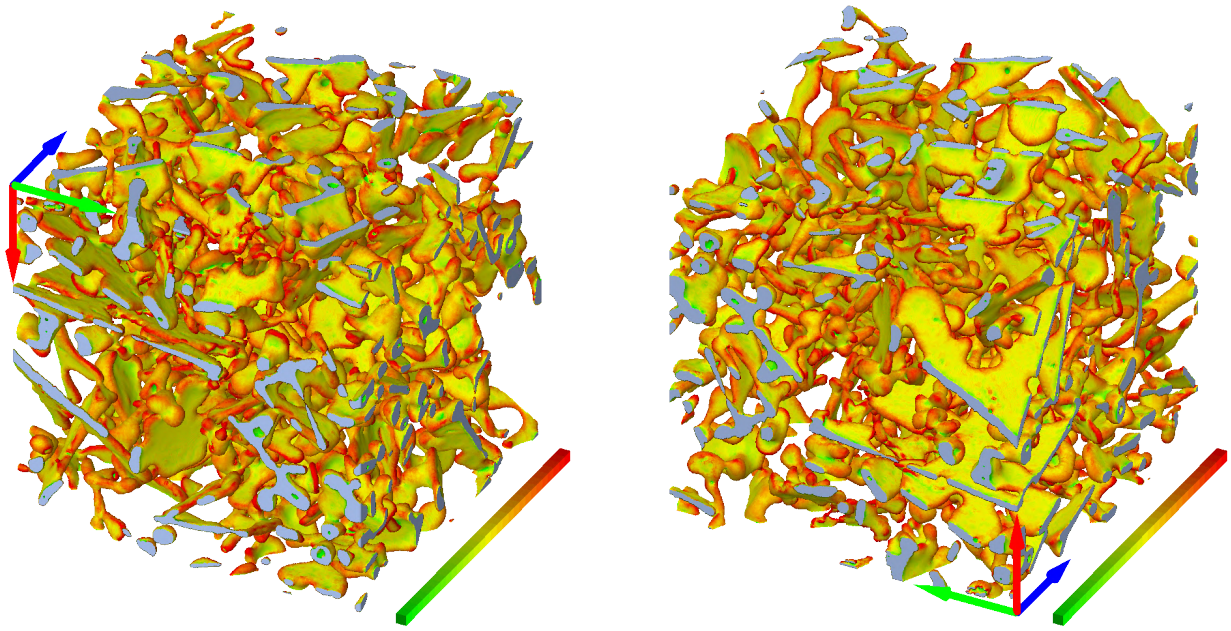

Figure S7. Downward (left) and upward (right) views of the whole image volume, where the mean local curvature is represented in each point of the surface. Concave surfaces are shown in green, convex surfaces in red, and flat surfaces in yellow (see colorbars from -30 to +30 mm^{-1}). The side of each viewing cube amounts to 2.95 mm. The blue, green, and red arrows, correspond to the x, y, and z coordinate axes, respectively.

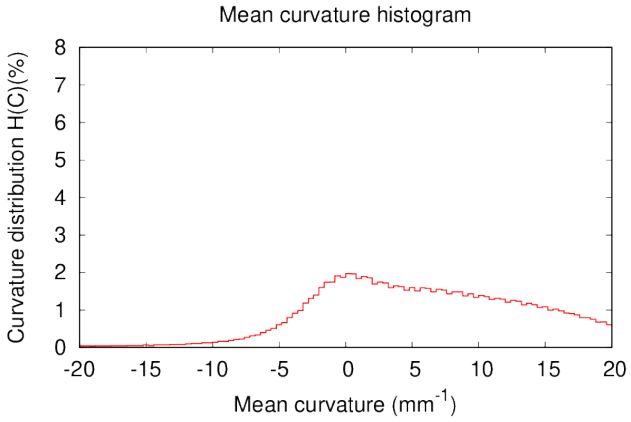

Figure S8. Mean curvature distribution on the whole image, from -20 to +20 mm^{-1}. Each bin is 0.4 mm^{-1} wide.

Image I08

Table S7.

Snow type	Image size (voxel)	Pixel size (µm)	ρ (kg m^{-3})	SSA (m^2 kg^{-1})	d (mm)	$\overline{\mathrm{MC}}$ (mm^{-1})	IQR$_{\mathrm{MC}}$ (mm^{-1})
DF	512	4.910	147.71	29.32	0.2232	5.27	8.80

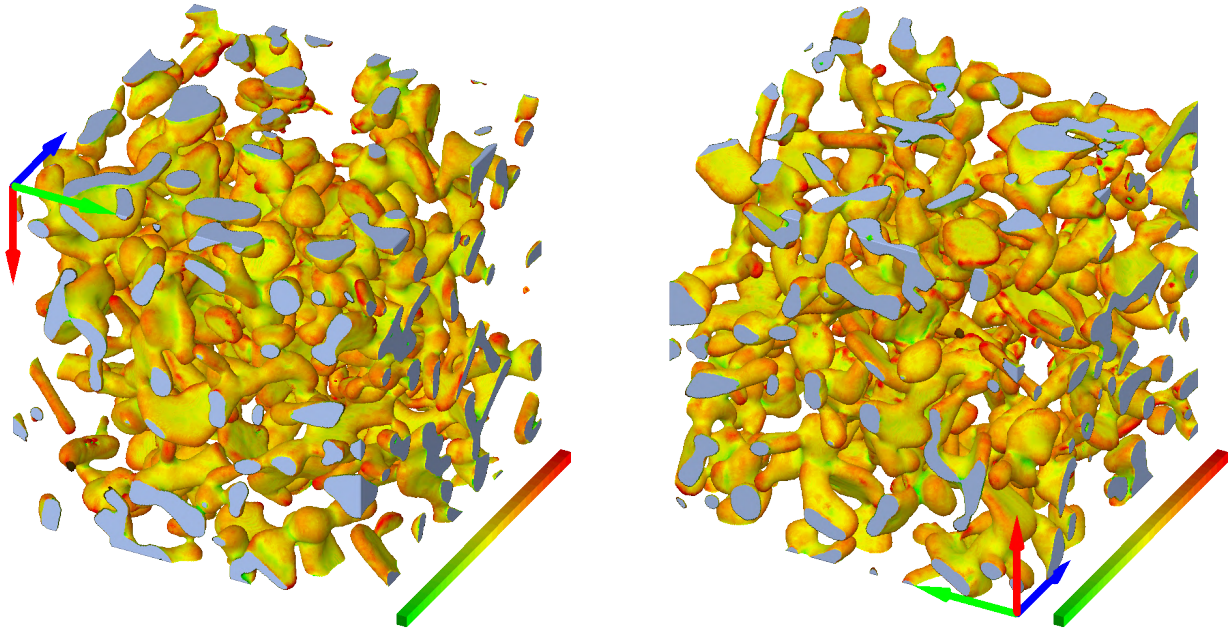

Figure S9. Downward (left) and upward (right) views of the whole image volume, where the mean local curvature is represented in each point of the surface. Concave surfaces are shown in green, convex surfaces in red, and flat surfaces in yellow (see colorbars from -30 to +30 mm^{-1}). The side of each viewing cube amounts to 2.51 mm. The blue, green, and red arrows, correspond to the x, y, and z coordinate axes, respectively.

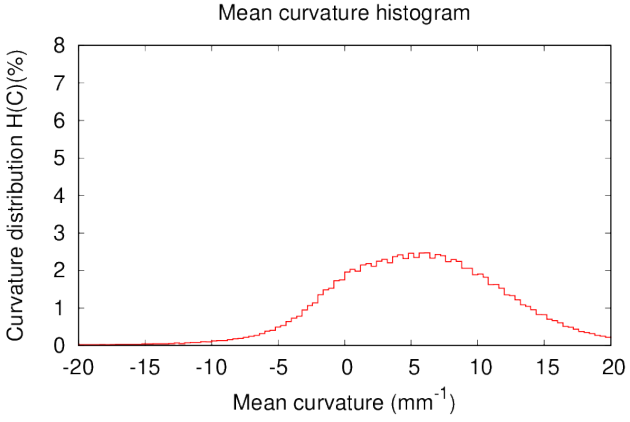

Figure S10. Mean curvature distribution on the whole image, from -20 to +20 mm^{-1}. Each bin is 0.4 mm^{-1} wide.

Image I15

Table S8.

Snow type	Image size (voxel)	Pixel size (µm)	ρ (kg m^{-3})	SSA (m^2 kg^{-1})	d (mm)	$\overline{\mathrm{MC}}$ (mm^{-1})	IQR$_{\mathrm{MC}}$ (mm^{-1})
RG	600	4.910	172.74	23.32	0.2805	4.10	6.54

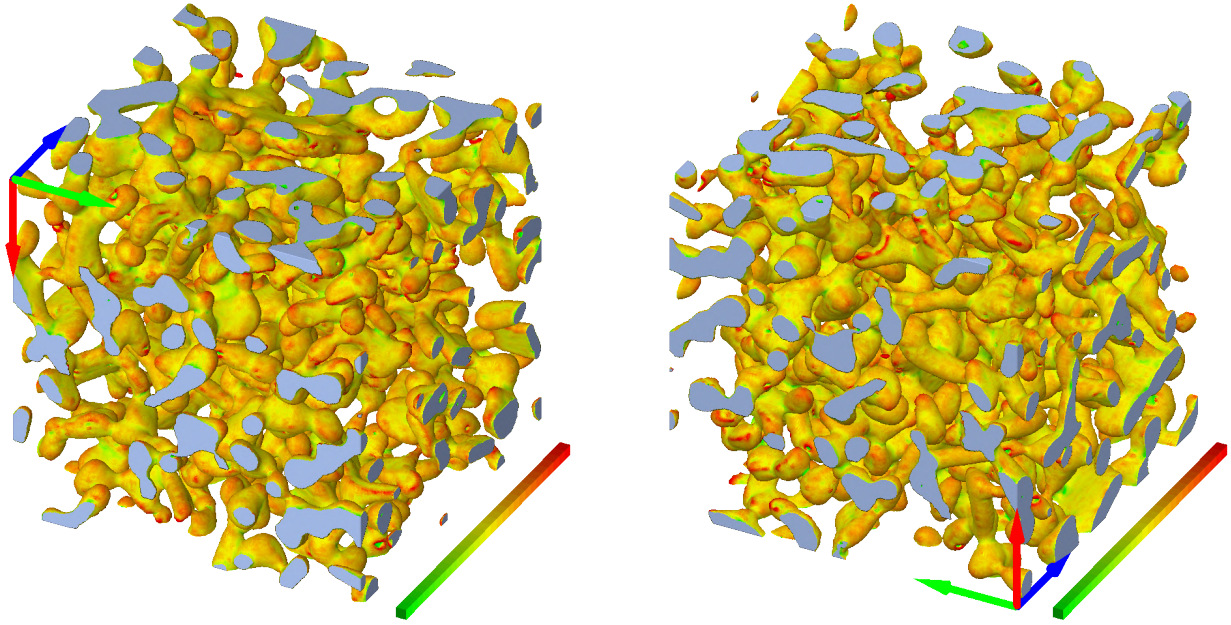

Figure S11. Downward (left) and upward (right) views of the whole image volume, where the mean local curvature is represented in each point of the surface. Concave surfaces are shown in green, convex surfaces in red, and flat surfaces in yellow (see colorbars from -30 to +30 mm^{-1}). The side of each viewing cube amounts to 2.95 mm. The blue, green, and red arrows, correspond to the x, y, and z coordinate axes, respectively.

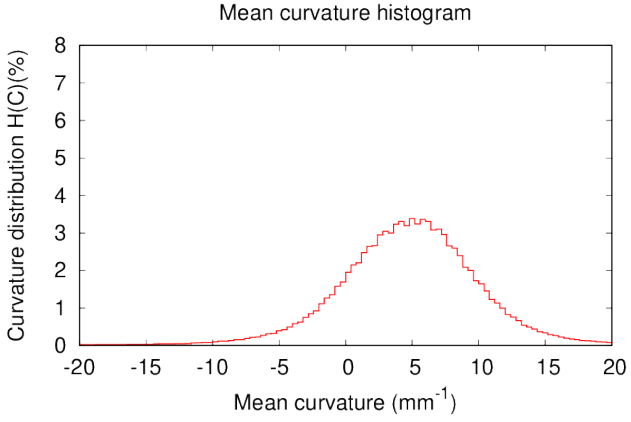

Figure S12. Mean curvature distribution on the whole image, from -20 to +20 mm^{-1}. Each bin is 0.4 mm^{-1} wide.

Image I19

Table S9.

Snow type	Image size (voxel)	Pixel size (µm)	ρ (kg m^{-3})	SSA (m^2 kg^{-1})	d (mm)	$\overline{\mathrm{MC}}$ (mm^{-1})	IQR$_{\mathrm{MC}}$ (mm^{-1})
RG	600	4.910	192.47	19.90	0.3288	3.47	5.80

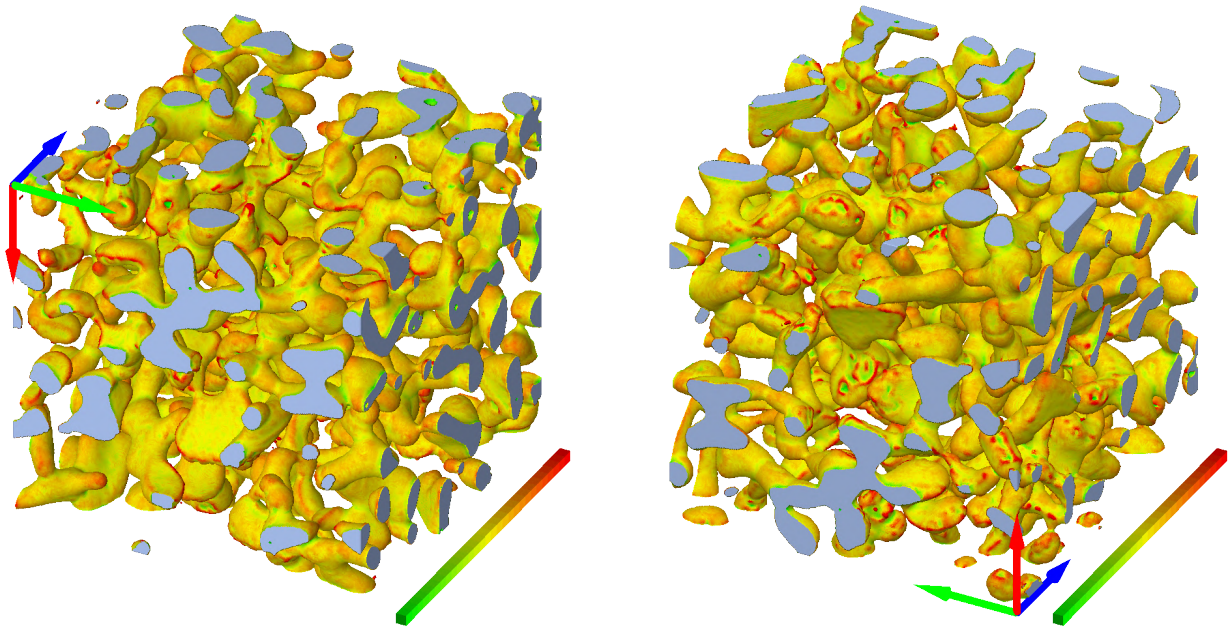

Figure S13. Downward (left) and upward (right) views of the whole image volume, where the mean local curvature is represented in each point of the surface. Concave surfaces are shown in green, convex surfaces in red, and flat surfaces in yellow (see colorbars from -30 to +30 mm^{-1}). The side of each viewing cube amounts to 2.95 mm. The blue, green, and red arrows, correspond to the x, y, and z coordinate axes, respectively.

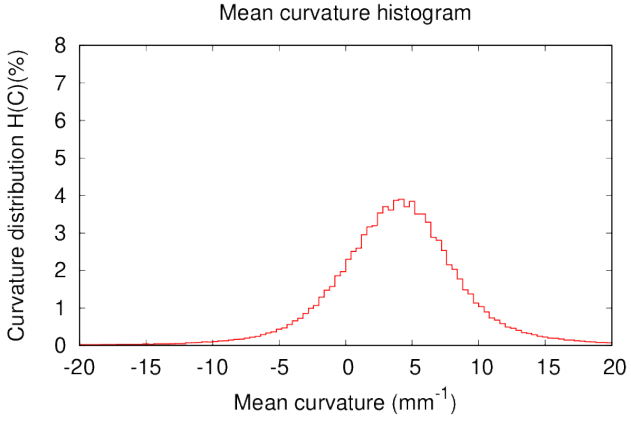

Figure S14. Mean curvature distribution on the whole image, from -20 to +20 mm^{-1}. Each bin is 0.4 mm^{-1} wide.

Image I21

Table S10.

Snow type	Image size (voxel)	Pixel size (µm)	ρ (kg m^{-3})	SSA (m^2 kg^{-1})	d (mm)	$\overline{\mathrm{MC}}$ (mm^{-1})	IQR$_{\mathrm{MC}}$ (mm^{-1})
RG	600	4.910	198.64	19.23	0.3402	3.28	5.58

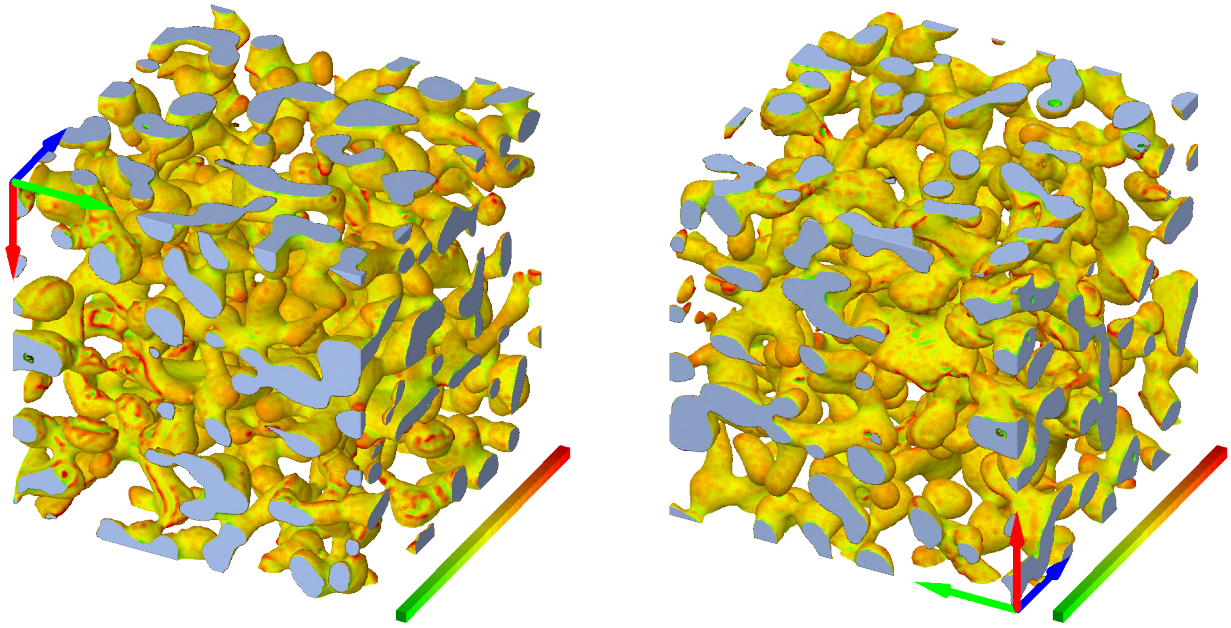

Figure S15. Downward (left) and upward (right) views of the whole image volume, where the mean local curvature is represented in each point of the surface. Concave surfaces are shown in green, convex surfaces in red, and flat surfaces in yellow (see colorbars from -30 to +30 mm^{-1}). The side of each viewing cube amounts to 2.95 mm. The blue, green, and red arrows, correspond to the x, y, and z coordinate axes, respectively.

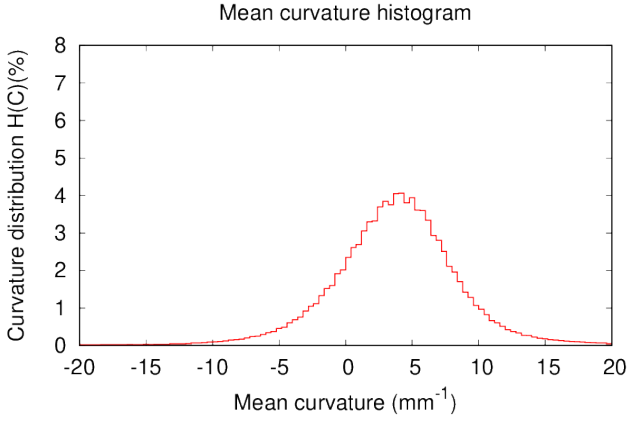

Figure S16. Mean curvature distribution on the whole image, from -20 to +20 mm^{-1}. Each bin is 0.4 mm^{-1} wide.

Image I23

Table S11.

Snow type	Image size (voxel)	Pixel size (µm)	ρ (kg m^{-3})	SSA (m^2 kg^{-1})	d (mm)	$\overline{\mathrm{MC}}$ (mm^{-1})	IQR$_{\mathrm{MC}}$ (mm^{-1})
RG	512	4.910	256.28	17.24	0.3804	2.54	4.75

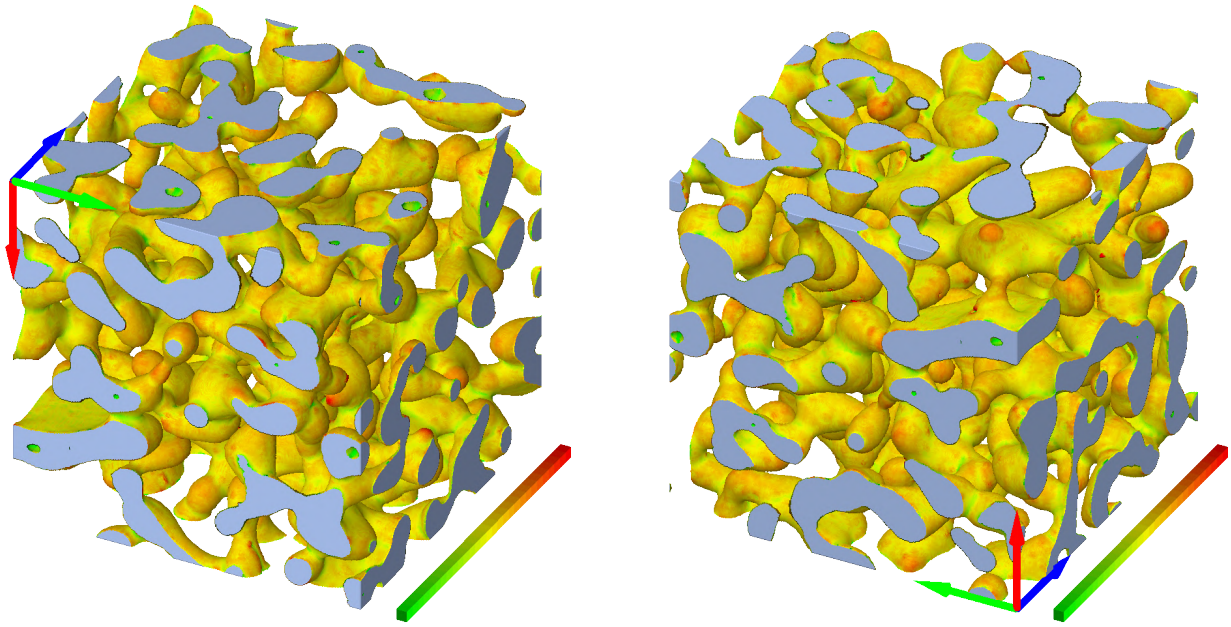

Figure S17. Downward (left) and upward (right) views of the whole image volume, where the mean local curvature is represented in each point of the surface. Concave surfaces are shown in green, convex surfaces in red, and flat surfaces in yellow (see colorbars from -30 to +30 mm^{-1}). The side of each viewing cube amounts to 2.51 mm. The blue, green, and red arrows, correspond to the x, y, and z coordinate axes, respectively.

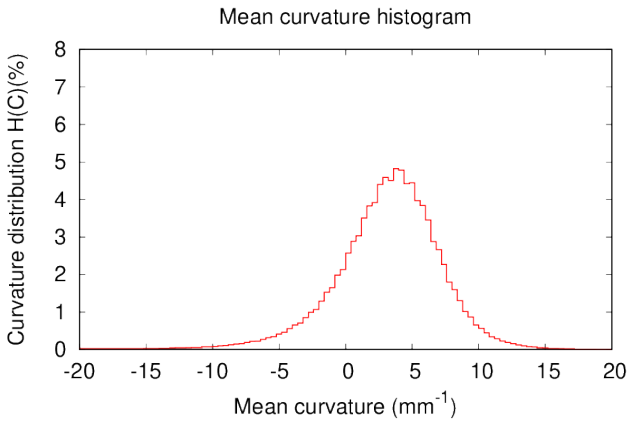

Figure S18. Mean curvature distribution on the whole image, from -20 to +20 mm^{-1}. Each bin is 0.4 mm^{-1} wide.

Image P03

Table S12.

Snow type	Image size (voxel)	Pixel size (µm)	ρ (kg m^{-3})	SSA (m^2 kg^{-1})	d (mm)	$\overline{\mathrm{MC}}$ (mm^{-1})	IQR$_{\mathrm{MC}}$ (mm^{-1})
PP	512	8.480	134.60	50.91	0.1285	13.16	14.99

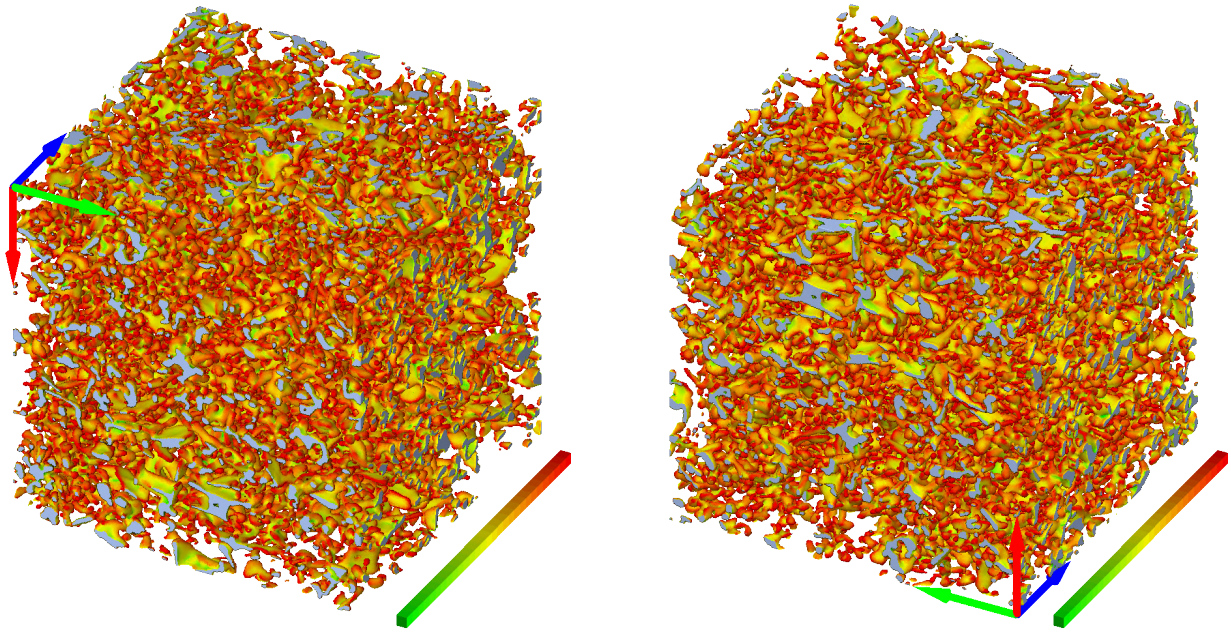

Figure S19. Downward (left) and upward (right) views of the whole image volume, where the mean local curvature is represented in each point of the surface. Concave surfaces are shown in green, convex surfaces in red, and flat surfaces in yellow (see colorbars from -30 to +30 mm^{-1}). The side of each viewing cube amounts to 4.34 mm. The blue, green, and red arrows, correspond to the x, y, and z coordinate axes, respectively.

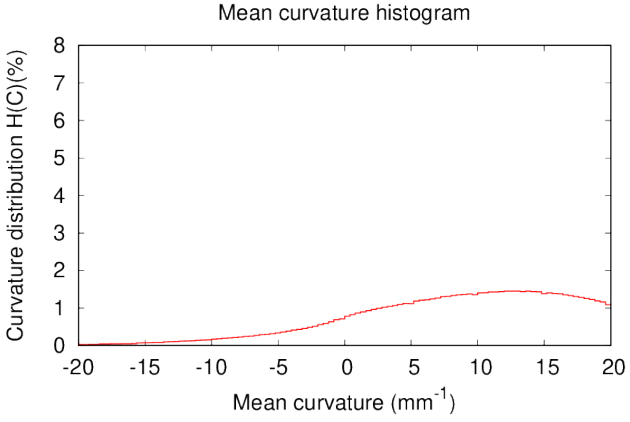

Figure S20. Mean curvature distribution on the whole image, from -20 to +20 mm^{-1}. Each bin is 0.4 mm^{-1} wide.

Image P04

Table S13.

Snow type	Image size (voxel)	Pixel size (µm)	ρ (kg m^{-3})	SSA (m^2 kg^{-1})	d (mm)	$\overline{\mathrm{MC}}$ (mm^{-1})	IQR$_{\mathrm{MC}}$ (mm^{-1})
DF	512	8.588	157.58	25.36	0.2580	5.10	7.08

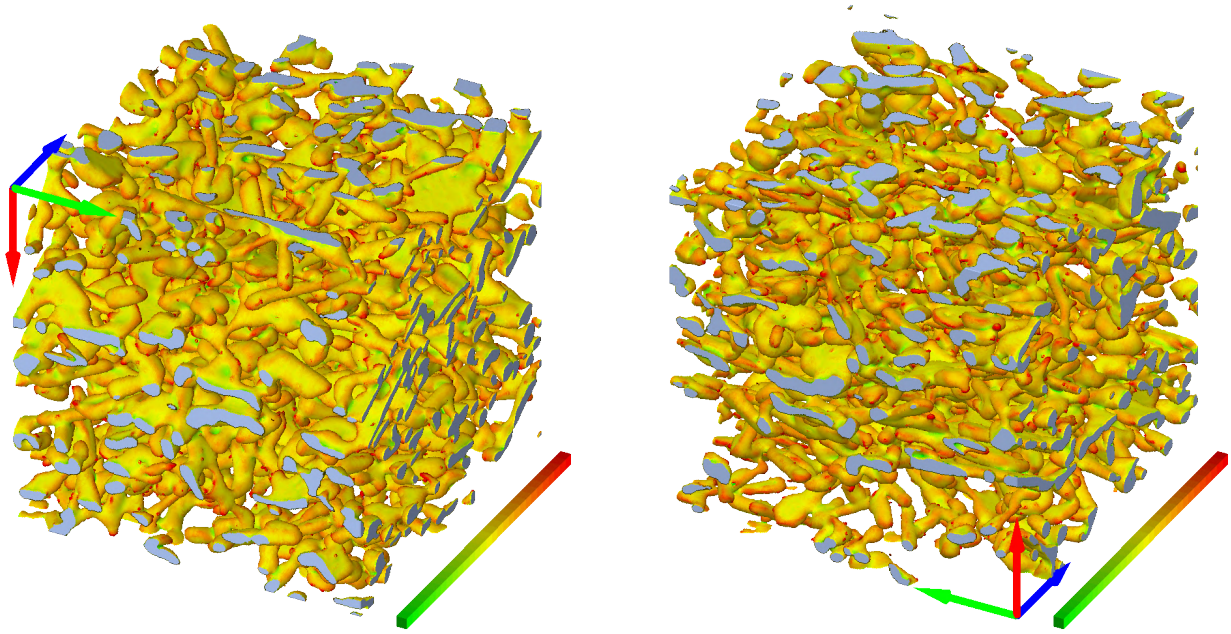

Figure S21. Downward (left) and upward (right) views of the whole image volume, where the mean local curvature is represented in each point of the surface. Concave surfaces are shown in green, convex surfaces in red, and flat surfaces in yellow (see colorbars from -30 to +30 mm^{-1}). The side of each viewing cube amounts to 4.40 mm. The blue, green, and red arrows, correspond to the x, y, and z coordinate axes, respectively.

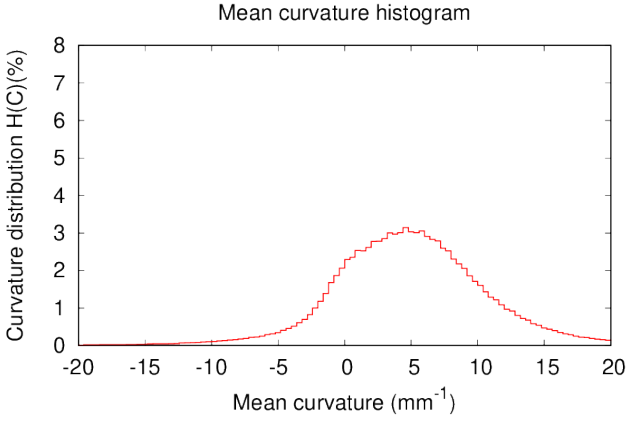

Figure S22. Mean curvature distribution on the whole image, from -20 to +20 mm^{-1}. Each bin is 0.4 mm^{-1} wide.

Image P06

Table S14.

Snow type	Image size (voxel)	Pixel size (µm)	ρ (kg m^{-3})	SSA (m^2 kg^{-1})	d (mm)	$\overline{\mathrm{MC}}$ (mm^{-1})	IQR$_{\mathrm{MC}}$ (mm^{-1})
RG	512	6.158	354.51	21.59	0.3031	3.30	6.45

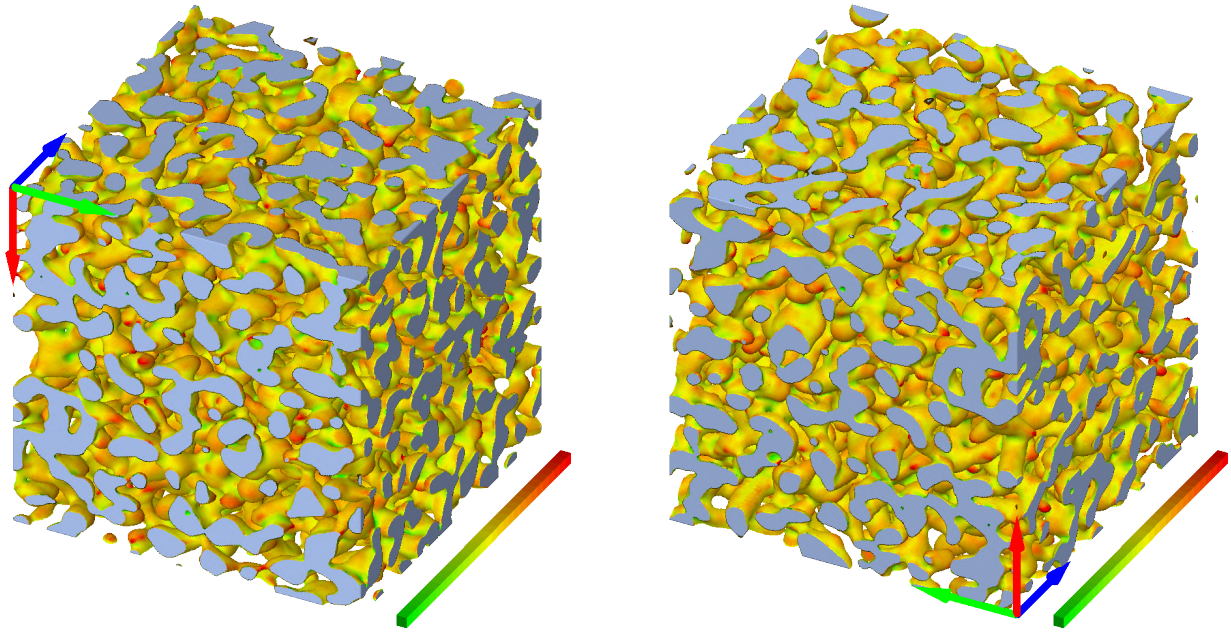

Figure S23. Downward (left) and upward (right) views of the whole image volume, where the mean local curvature is represented in each point of the surface. Concave surfaces are shown in green, convex surfaces in red, and flat surfaces in yellow (see colorbars from -30 to +30 mm^{-1}). The side of each viewing cube amounts to 3.15 mm. The blue, green, and red arrows, correspond to the x, y, and z coordinate axes, respectively.

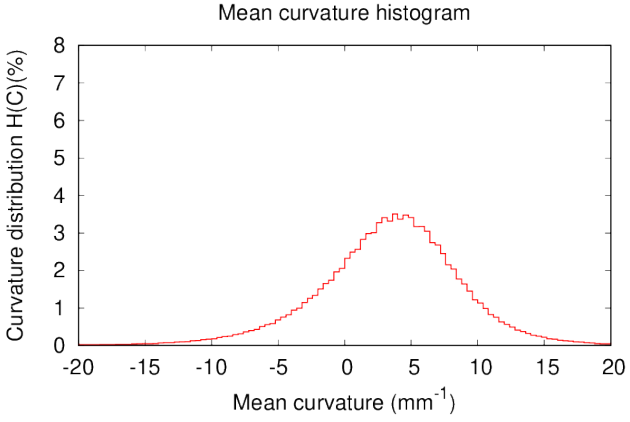

Figure S24. Mean curvature distribution on the whole image, from -20 to +20 mm^{-1}. Each bin is 0.4 mm^{-1} wide.

Image P07

Table S15.

Snow type	Image size (voxel)	Pixel size (µm)	ρ (kg m^{-3})	SSA (m^2 kg^{-1})	d (mm)	$\overline{\mathrm{MC}}$ (mm^{-1})	IQR$_{\mathrm{MC}}$ (mm^{-1})
RG	512	8.609	280.07	17.15	0.3816	3.01	5.29

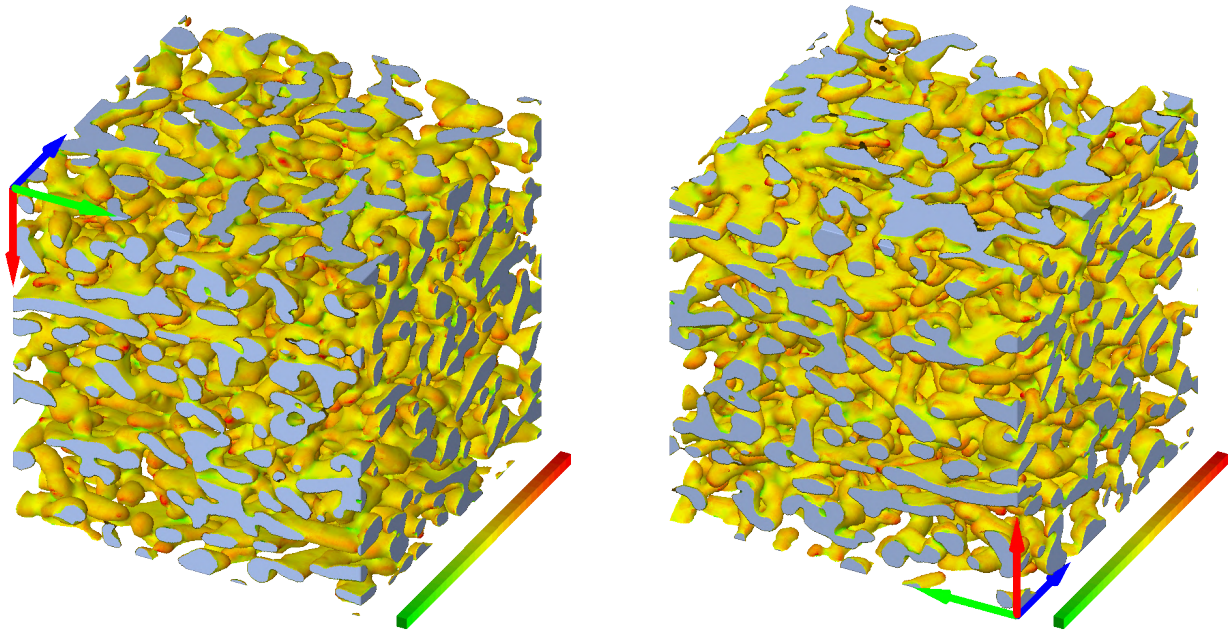

Figure S25. Downward (left) and upward (right) views of the whole image volume, where the mean local curvature is represented in each point of the surface. Concave surfaces are shown in green, convex surfaces in red, and flat surfaces in yellow (see colorbars from -30 to +30 mm^{-1}). The side of each viewing cube amounts to 4.41 mm. The blue, green, and red arrows, correspond to the x, y, and z coordinate axes, respectively.

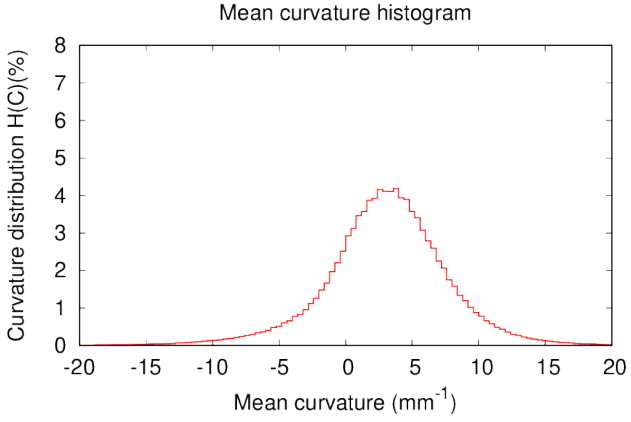

Figure S26. Mean curvature distribution on the whole image, from -20 to +20 mm^{-1}. Each bin is 0.4 mm^{-1} wide.

Image P08

Table S16.

Snow type	Image size (voxel)	Pixel size (µm)	ρ (kg m^{-3})	SSA (m^2 kg^{-1})	d (mm)	$\overline{\mathrm{MC}}$ (mm^{-1})	IQR$_{\mathrm{MC}}$ (mm^{-1})
RG	512	8.552	378.96	14.57	0.4490	1.85	4.84

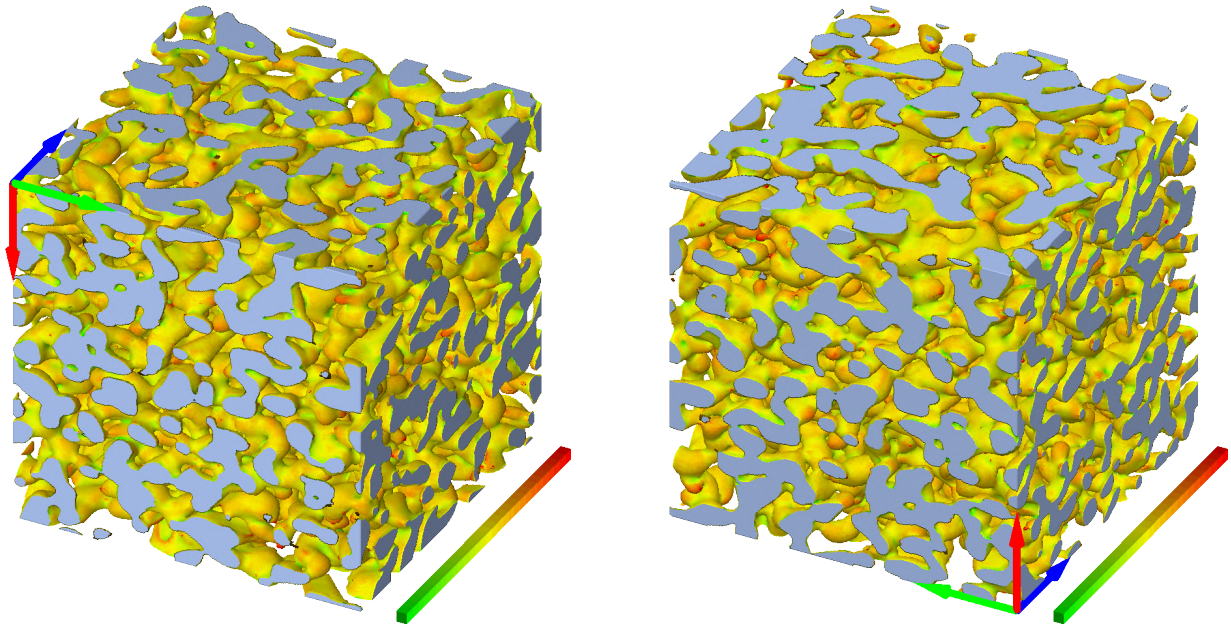

Figure S27. Downward (left) and upward (right) views of the whole image volume, where the mean local curvature is represented in each point of the surface. Concave surfaces are shown in green, convex surfaces in red, and flat surfaces in yellow (see colorbars from -30 to +30 mm^{-1}). The side of each viewing cube amounts to 4.38 mm. The blue, green, and red arrows, correspond to the x, y, and z coordinate axes, respectively.

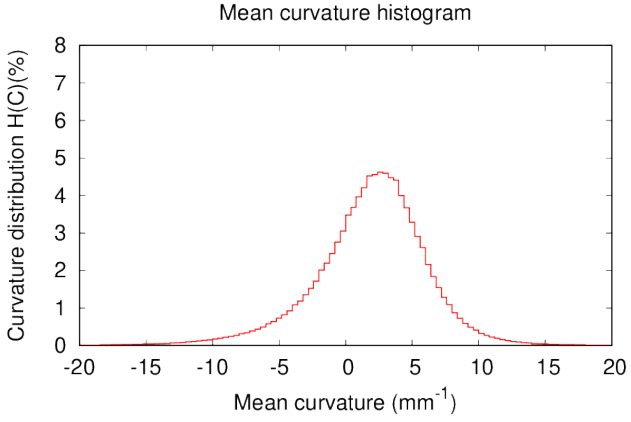

Figure S28. Mean curvature distribution on the whole image, from -20 to +20 mm^{-1}. Each bin is 0.4 mm^{-1} wide.

Image P09

Table S17.

Snow type	Image size (voxel)	Pixel size (µm)	ρ (kg m^{-3})	SSA (m^2 kg^{-1})	d (mm)	$\overline{\mathrm{MC}}$ (mm^{-1})	IQR$_{\mathrm{MC}}$ (mm^{-1})
RG	512	6.158	396.13	12.29	0.5325	1.61	5.15

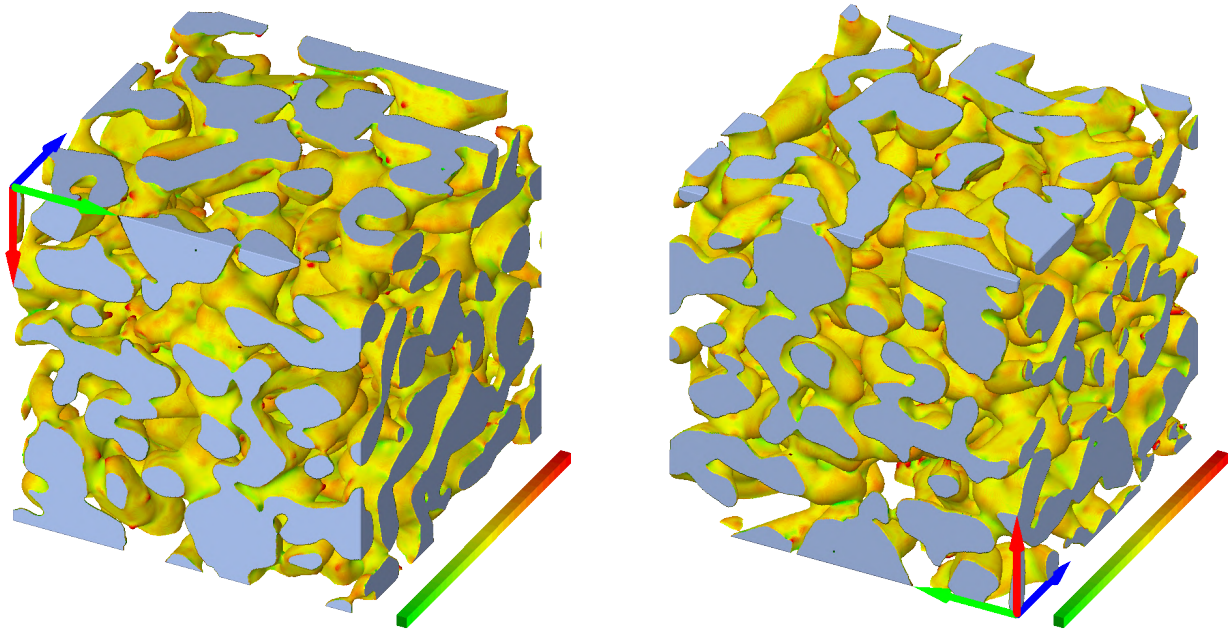

Figure S29. Downward (left) and upward (right) views of the whole image volume, where the mean local curvature is represented in each point of the surface. Concave surfaces are shown in green, convex surfaces in red, and flat surfaces in yellow (see colorbars from -30 to +30 mm^{-1}). The side of each viewing cube amounts to 3.15 mm. The blue, green, and red arrows, correspond to the x, y, and z coordinate axes, respectively.

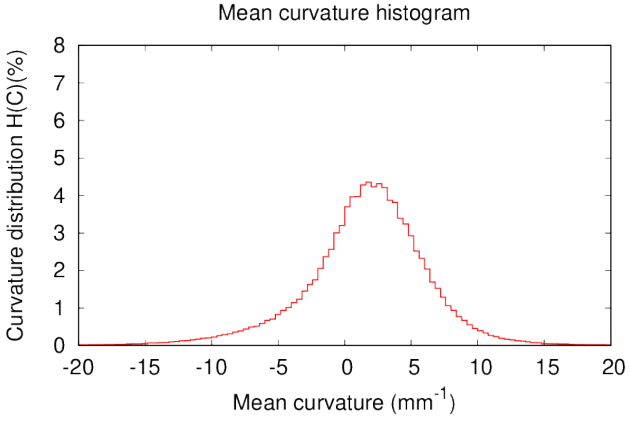

Figure S30. Mean curvature distribution on the whole image, from -20 to +20 mm^{-1}. Each bin is 0.4 mm^{-1} wide.

Image P10

Table S18.

Snow type	Image size (voxel)	Pixel size (µm)	ρ (kg m^{-3})	SSA (m^2 kg^{-1})	d (mm)	$\overline{\mathrm{MC}}$ (mm^{-1})	IQR$_{\mathrm{MC}}$ (mm^{-1})
RG	512	6.103	396.07	10.46	0.6253	1.25	4.78

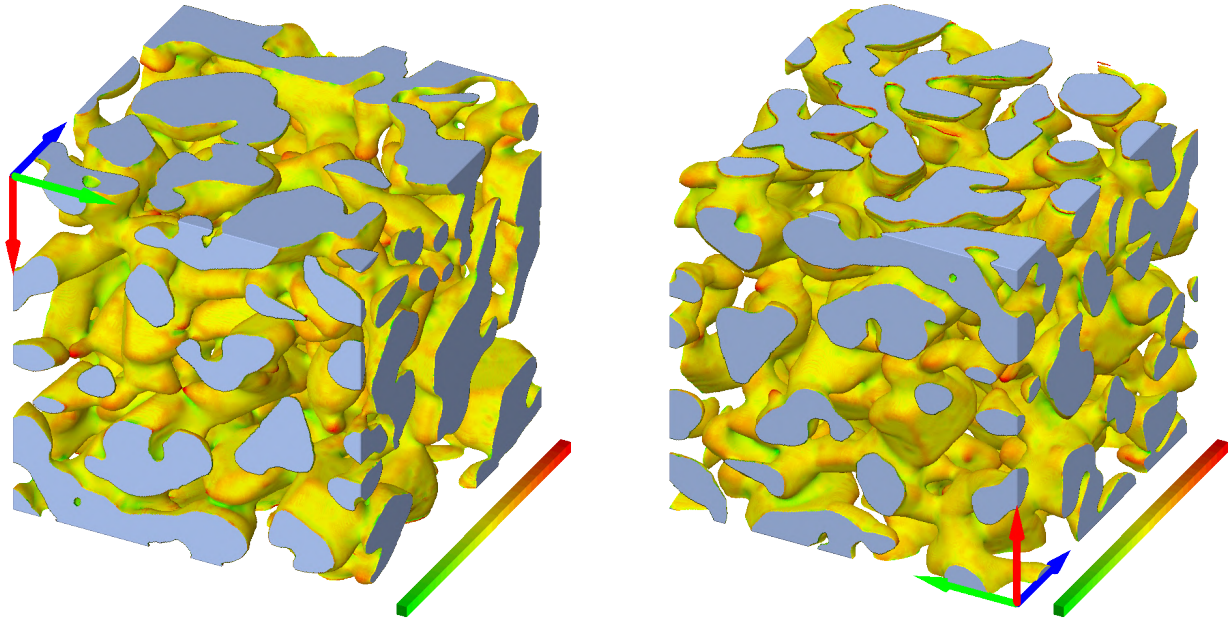

Figure S31. Downward (left) and upward (right) views of the whole image volume, where the mean local curvature is represented in each point of the surface. Concave surfaces are shown in green, convex surfaces in red, and flat surfaces in yellow (see colorbars from -30 to +30 mm^{-1}). The side of each viewing cube amounts to 3.12 mm. The blue, green, and red arrows, correspond to the x, y, and z coordinate axes, respectively.

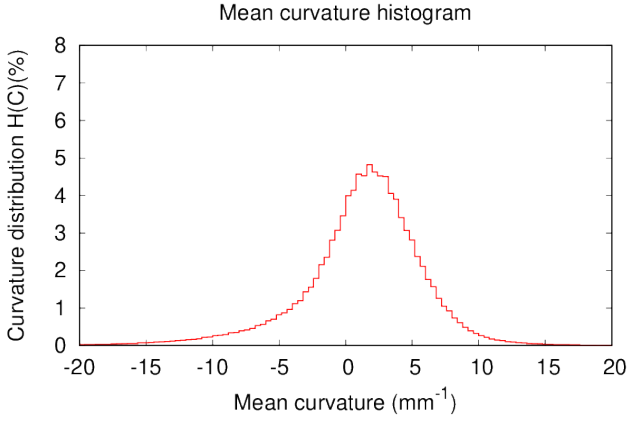

Figure S32. Mean curvature distribution on the whole image, from -20 to +20 mm^{-1}. Each bin is 0.4 mm^{-1} wide.

Image P11

Table S19.

Snow type	Image size (voxel)	Pixel size (µm)	ρ (kg m^{-3})	SSA (m^2 kg^{-1})	d (mm)	$\overline{\mathrm{MC}}$ (mm^{-1})	IQR$_{\mathrm{MC}}$ (mm^{-1})
RG	512	8.588	413.71	20.76	0.3151	3.13	7.18

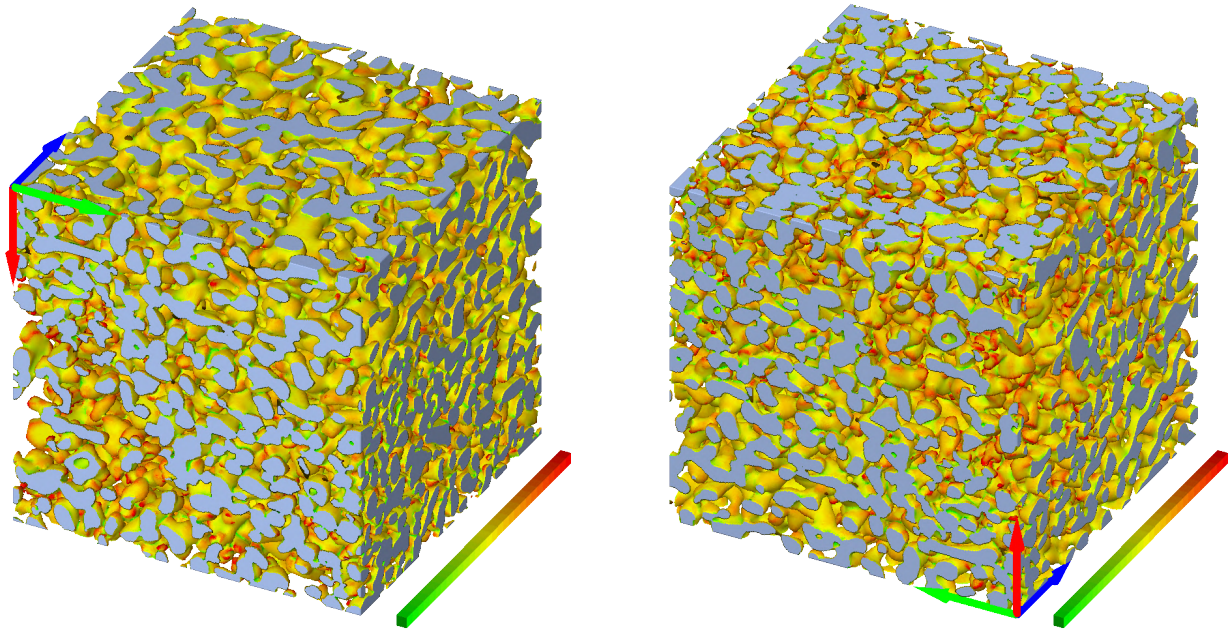

Figure S33. Downward (left) and upward (right) views of the whole image volume, where the mean local curvature is represented in each point of the surface. Concave surfaces are shown in green, convex surfaces in red, and flat surfaces in yellow (see colorbars from -30 to +30 mm^{-1}). The side of each viewing cube amounts to 4.40 mm. The blue, green, and red arrows, correspond to the x, y, and z coordinate axes, respectively.

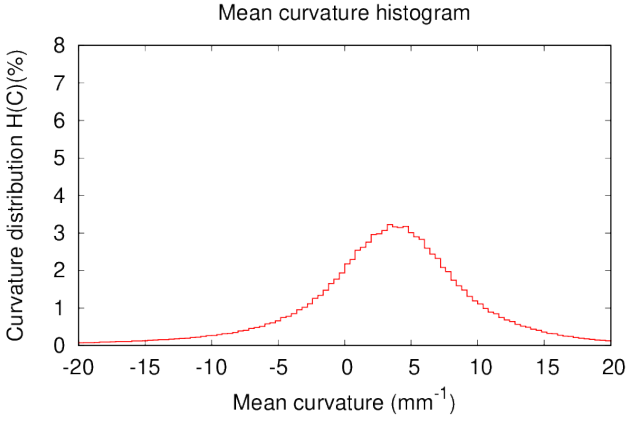

Figure S34. Mean curvature distribution on the whole image, from -20 to +20 mm^{-1}. Each bin is 0.4 mm^{-1} wide.

Image P14

Table S20.

Snow type	Image size (voxel)	Pixel size (µm)	ρ (kg m^{-3})	SSA (m^2 kg^{-1})	d (mm)	$\overline{\mathrm{MC}}$ (mm^{-1})	IQR$_{\mathrm{MC}}$ (mm^{-1})
RG	600	6.154	359.84	18.13	0.3608	2.35	6.86

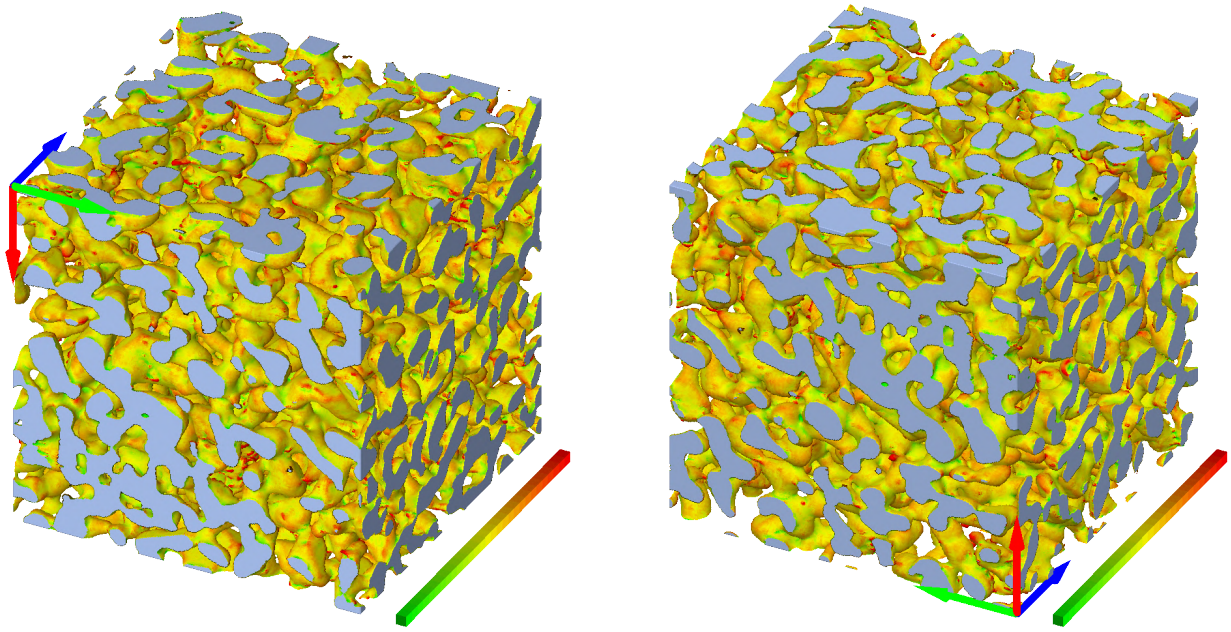

Figure S35. Downward (left) and upward (right) views of the whole image volume, where the mean local curvature is represented in each point of the surface. Concave surfaces are shown in green, convex surfaces in red, and flat surfaces in yellow (see colorbars from -30 to +30 mm^{-1}). The side of each viewing cube amounts to 3.69 mm. The blue, green, and red arrows, correspond to the x, y, and z coordinate axes, respectively.

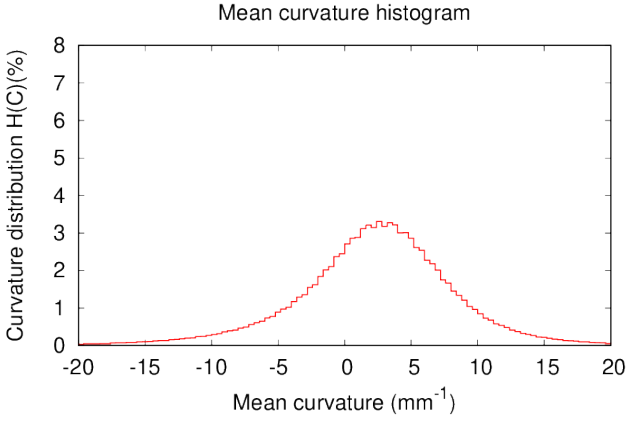

Figure S36. Mean curvature distribution on the whole image, from -20 to +20 mm^{-1}. Each bin is 0.4 mm^{-1} wide.

Image P15

Table S21.

Snow type	Image size (voxel)	Pixel size (µm)	ρ (kg m^{-3})	SSA (m^2 kg^{-1})	d (mm)	$\overline{\mathrm{MC}}$ (mm^{-1})	IQR$_{\mathrm{MC}}$ (mm^{-1})
RG	512	6.158	315.50	16.09	0.4067	2.65	5.65

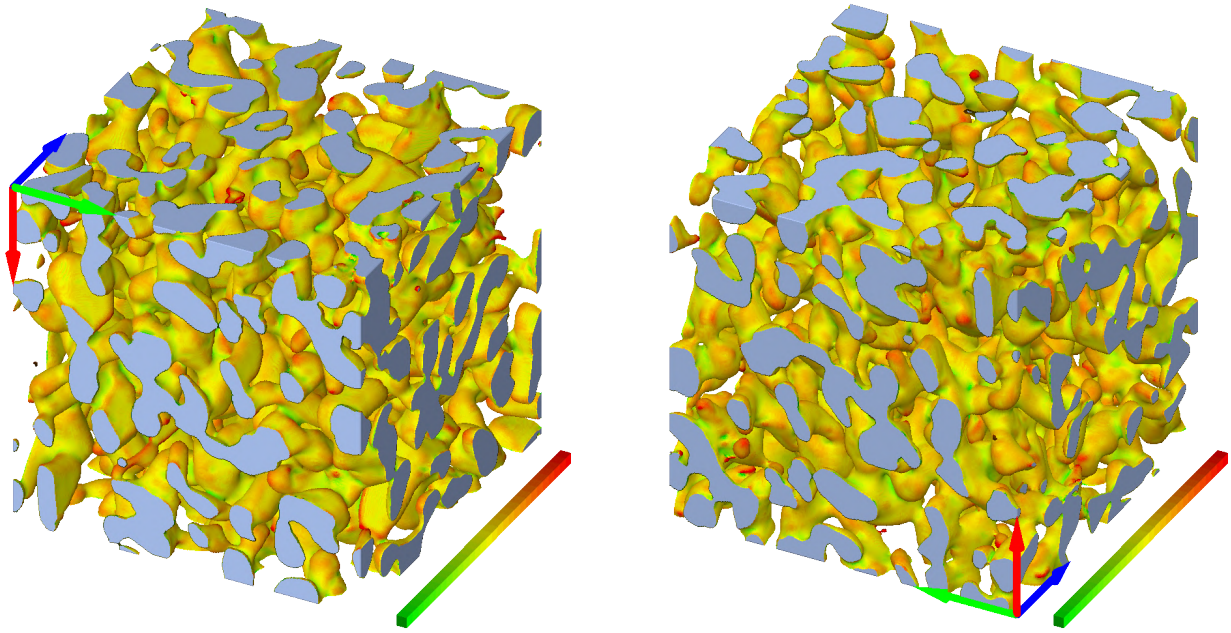

Figure S37. Downward (left) and upward (right) views of the whole image volume, where the mean local curvature is represented in each point of the surface. Concave surfaces are shown in green, convex surfaces in red, and flat surfaces in yellow (see colorbars from -30 to +30 mm^{-1}). The side of each viewing cube amounts to 3.15 mm. The blue, green, and red arrows, correspond to the x, y, and z coordinate axes, respectively.

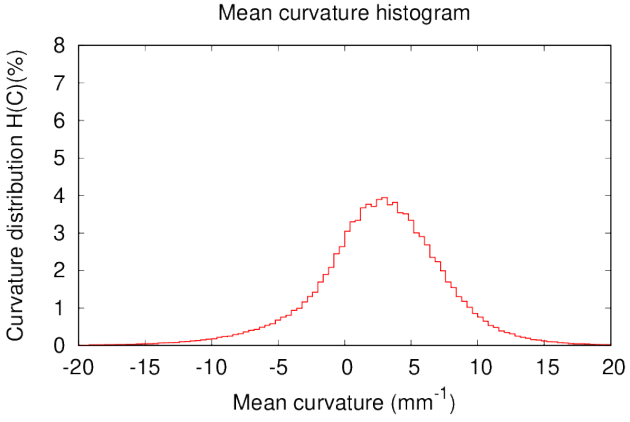

Figure S38. Mean curvature distribution on the whole image, from -20 to +20 mm^{-1}. Each bin is 0.4 mm^{-1} wide.

Image NH0

Table S22.

Snow type	Image size (voxel)	Pixel size (µm)	ρ (kg m^{-3})	SSA (m^2 kg^{-1})	d (mm)	$\overline{\mathrm{MC}}$ (mm^{-1})	IQR$_{\mathrm{MC}}$ (mm^{-1})
RG	651	8.609	430.59	17.34	0.3773	2.37	6.61

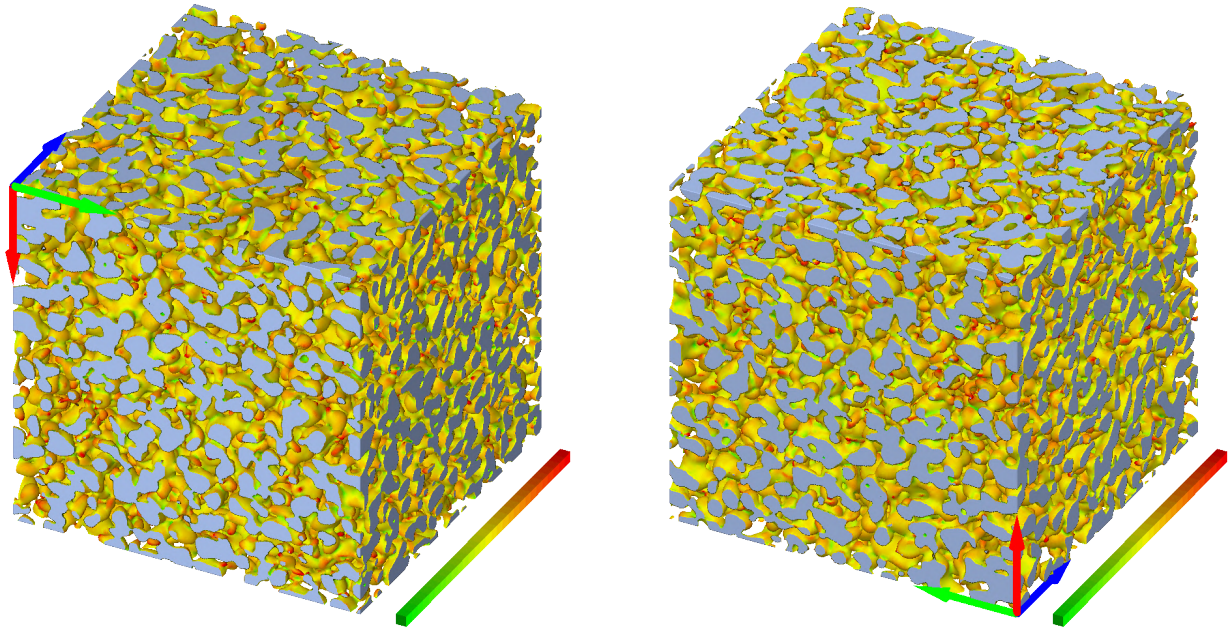

Figure S39. Downward (left) and upward (right) views of the whole image volume, where the mean local curvature is represented in each point of the surface. Concave surfaces are shown in green, convex surfaces in red, and flat surfaces in yellow (see colorbars from -30 to +30 mm^{-1}). The side of each viewing cube amounts to 5.60 mm. The blue, green, and red arrows, correspond to the x, y, and z coordinate axes, respectively.

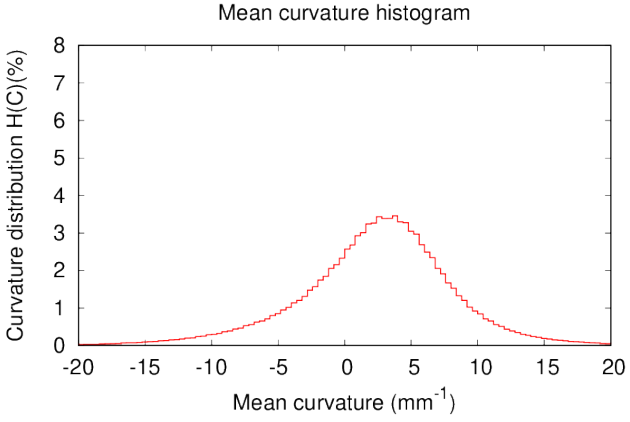

Figure S40. Mean curvature distribution on the whole image, from -20 to +20 mm^{-1}. Each bin is 0.4 mm^{-1} wide.

Image NH1

Table S23.

Snow type	Image size (voxel)	Pixel size (µm)	ρ (kg m^{-3})	SSA (m^2 kg^{-1})	d (mm)	$\overline{\mathrm{MC}}$ (mm^{-1})	IQR$_{\mathrm{MC}}$ (mm^{-1})
MF	651	8.609	544.08	6.99	0.9363	-0.05	8.10

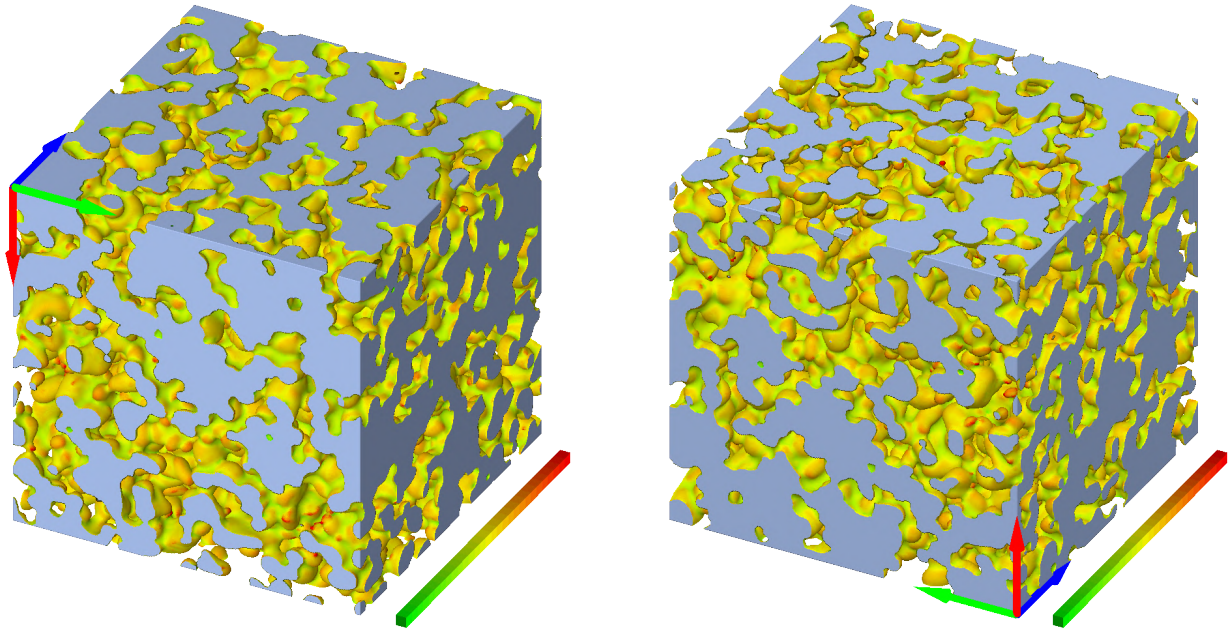

Figure S41. Downward (left) and upward (right) views of the whole image volume, where the mean local curvature is represented in each point of the surface. Concave surfaces are shown in green, convex surfaces in red, and flat surfaces in yellow (see colorbars from -30 to +30 mm^{-1}). The side of each viewing cube amounts to 5.60 mm. The blue, green, and red arrows, correspond to the x, y, and z coordinate axes, respectively.

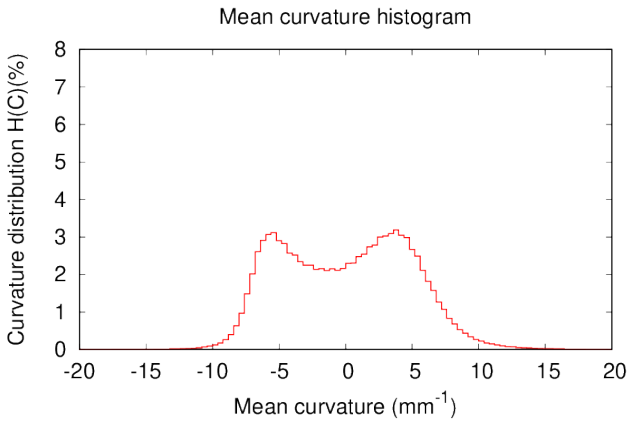

Figure S42. Mean curvature distribution on the whole image, from -20 to +20 mm^{-1}. Each bin is 0.4 mm^{-1} wide.

Image NH12

Table S24.

Snow type	Image size (voxel)	Pixel size (µm)	ρ (kg m^{-3})	SSA (m^2 kg^{-1})	d (mm)	$\overline{\mathrm{MC}}$ (mm^{-1})	IQR$_{\mathrm{MC}}$ (mm^{-1})
MF	651	8.590	512.89	7.69	0.8514	0.14	6.82

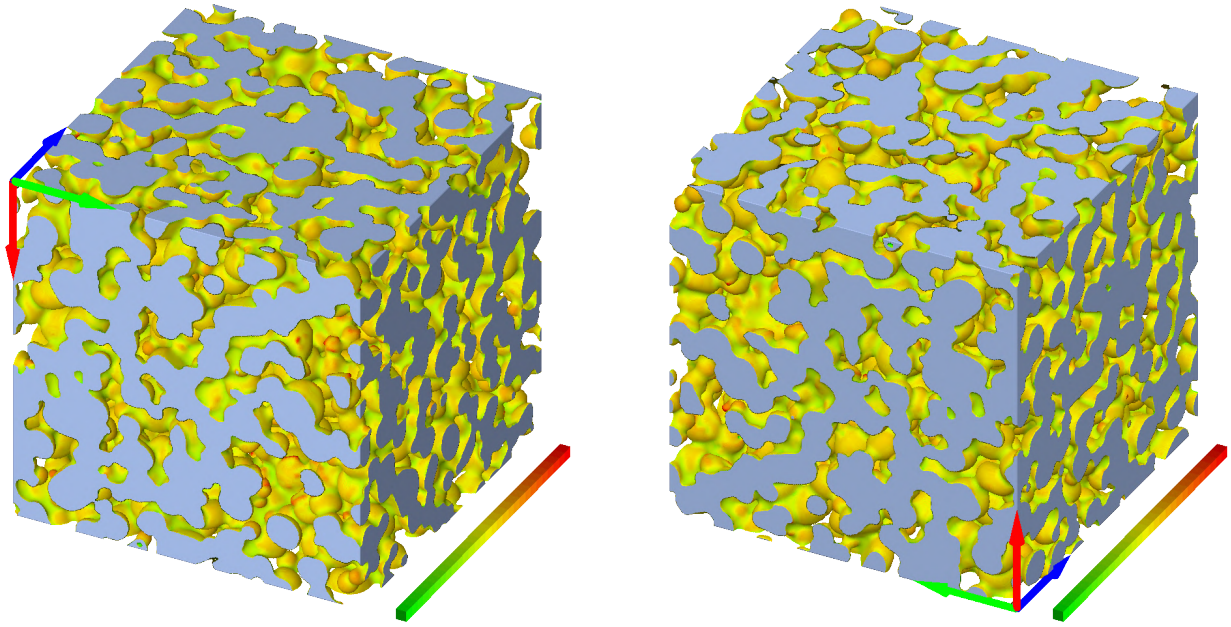

Figure S43. Downward (left) and upward (right) views of the whole image volume, where the mean local curvature is represented in each point of the surface. Concave surfaces are shown in green, convex surfaces in red, and flat surfaces in yellow (see colorbars from -30 to +30 mm^{-1}). The side of each viewing cube amounts to 5.59 mm. The blue, green, and red arrows, correspond to the x, y, and z coordinate axes, respectively.

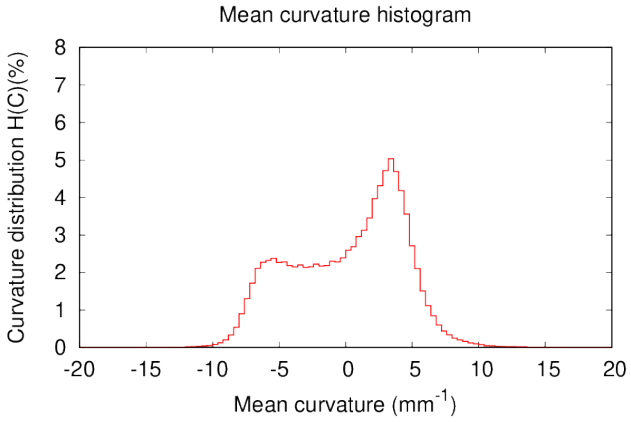

Figure S44. Mean curvature distribution on the whole image, from -20 to +20 mm^{-1}. Each bin is 0.4 mm^{-1} wide.

Image NH2

Table S25.

Snow type	Image size (voxel)	Pixel size (µm)	ρ (kg m^{-3})	SSA (m^2 kg^{-1})	d (mm)	$\overline{\mathrm{MC}}$ (mm^{-1})	IQR$_{\mathrm{MC}}$ (mm^{-1})
MF	651	8.590	502.60	6.18	1.0584	0.31	5.15

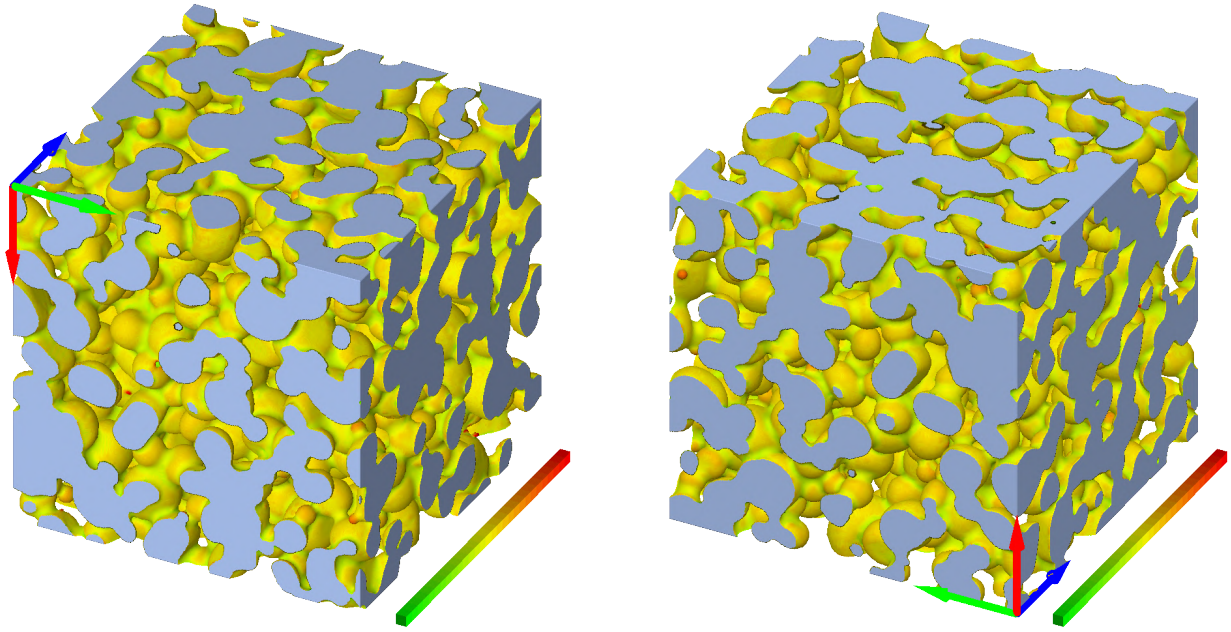

Figure S45. Downward (left) and upward (right) views of the whole image volume, where the mean local curvature is represented in each point of the surface. Concave surfaces are shown in green, convex surfaces in red, and flat surfaces in yellow (see colorbars from -30 to +30 mm^{-1}). The side of each viewing cube amounts to 5.59 mm. The blue, green, and red arrows, correspond to the x, y, and z coordinate axes, respectively.

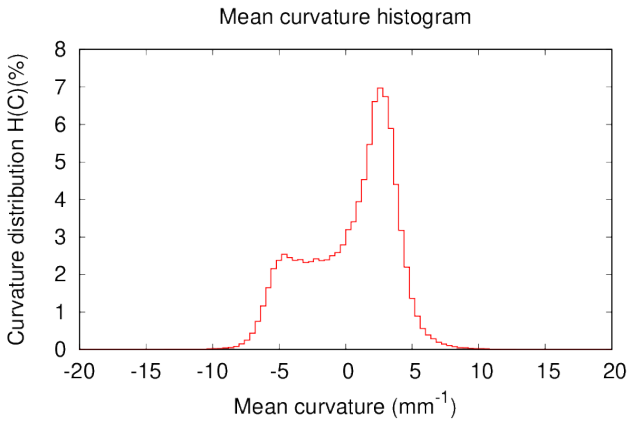

Figure S46. Mean curvature distribution on the whole image, from -20 to +20 mm^{-1}. Each bin is 0.4 mm^{-1} wide.

Image NH5

Table S26.

Snow type	Image size (voxel)	Pixel size (µm)	ρ (kg m^{-3})	SSA (m^2 kg^{-1})	d (mm)	$\overline{\mathrm{MC}}$ (mm^{-1})	IQR$_{\mathrm{MC}}$ (mm^{-1})
MF	1000	9.460	472.83	3.78	1.7302	0.35	3.08

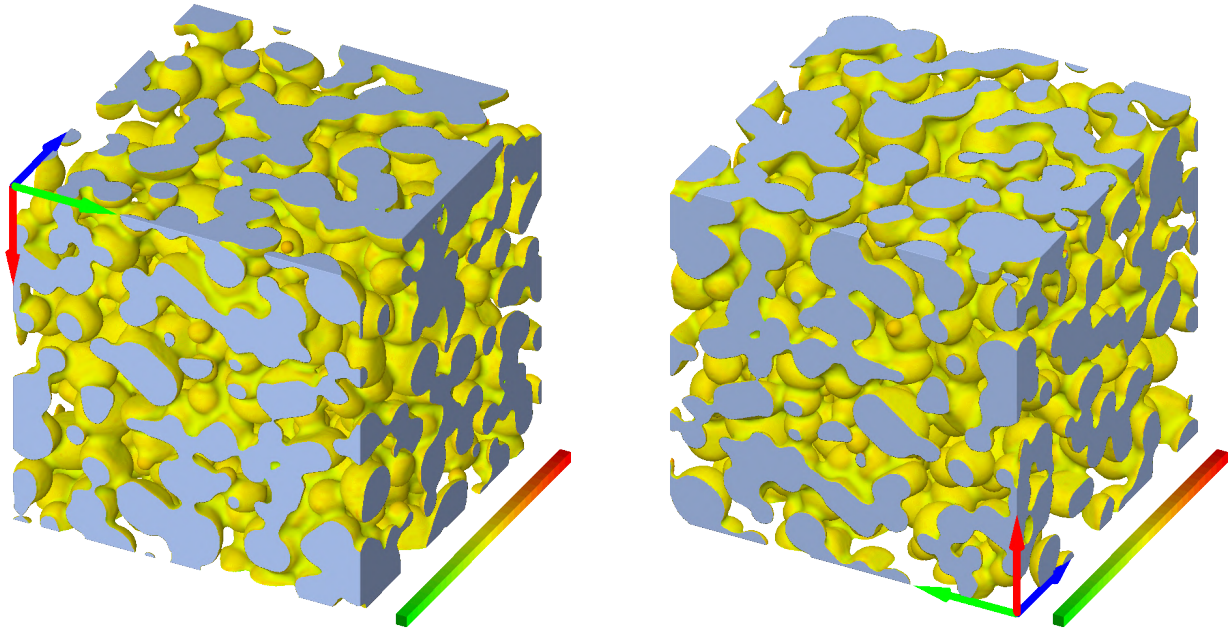

Figure S47. Downward (left) and upward (right) views of the whole image volume, where the mean local curvature is represented in each point of the surface. Concave surfaces are shown in green, convex surfaces in red, and flat surfaces in yellow (see colorbars from -30 to +30 mm^{-1}). The side of each viewing cube amounts to 9.46 mm. The blue, green, and red arrows, correspond to the x, y, and z coordinate axes, respectively.

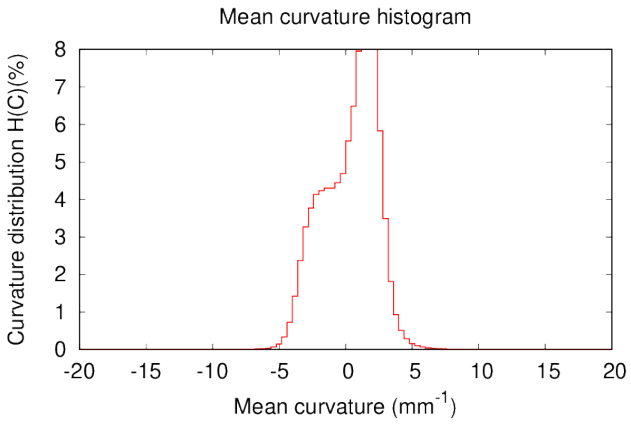

Figure S48. Mean curvature distribution on the whole image, from -20 to +20 mm^{-1}. Each bin is 0.4 mm^{-1} wide.

Image cham

Table S27.

Snow type	Image size (voxel)	Pixel size (µm)	ρ (kg m^{-3})	SSA (m^2 kg^{-1})	d (mm)	$\overline{\mathrm{MC}}$ (mm^{-1})	IQR$_{\mathrm{MC}}$ (mm^{-1})
MF	542	10.000	522.31	8.49	0.7702	0.13	6.90

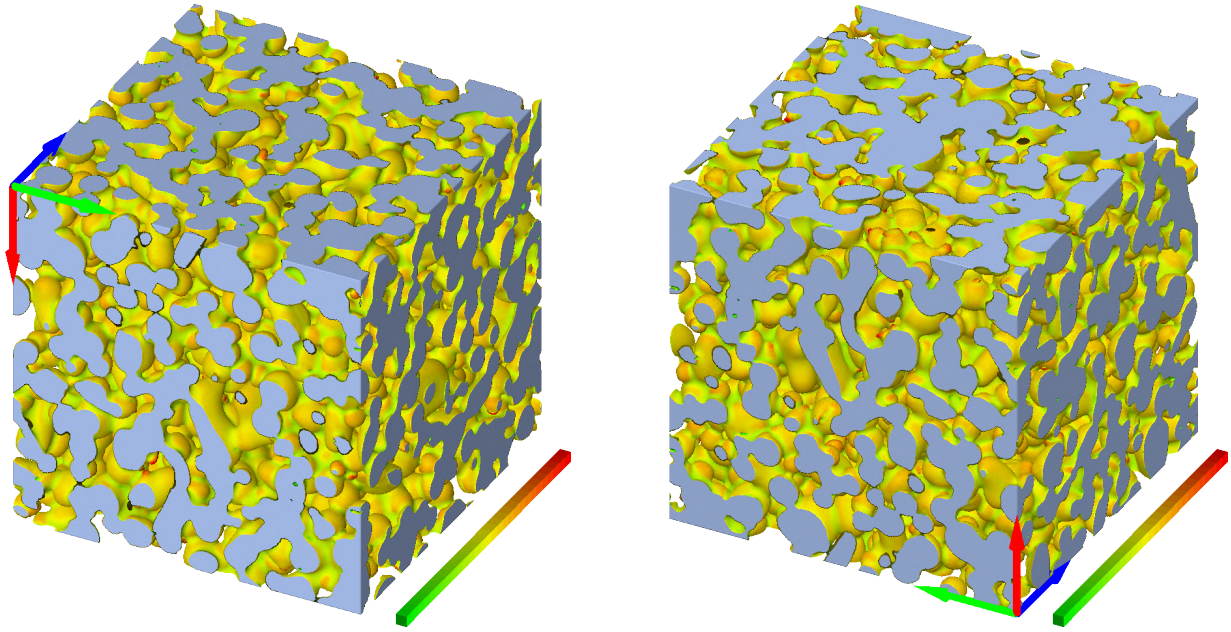

Figure S49. Downward (left) and upward (right) views of the whole image volume, where the mean local curvature is represented in each point of the surface. Concave surfaces are shown in green, convex surfaces in red, and flat surfaces in yellow (see colorbars from -30 to +30 mm^{-1}). The side of each viewing cube amounts to 5.42 mm. The blue, green, and red arrows, correspond to the x, y, and z coordinate axes, respectively.

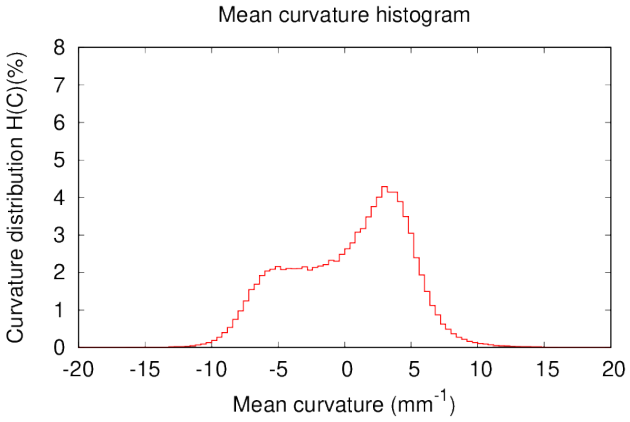

Figure S50. Mean curvature distribution on the whole image, from -20 to +20 mm^{-1}. Each bin is 0.4 mm^{-1} wide.

Image E2b

Table S28.

Snow type	Image size (voxel)	Pixel size (µm)	ρ (kg m^{-3})	SSA (m^2 kg^{-1})	d (mm)	$\overline{\mathrm{MC}}$ (mm^{-1})	IQR$_{\mathrm{MC}}$ (mm^{-1})
FC	1200	4.910	262.74	15.43	0.4240	1.99	7.64

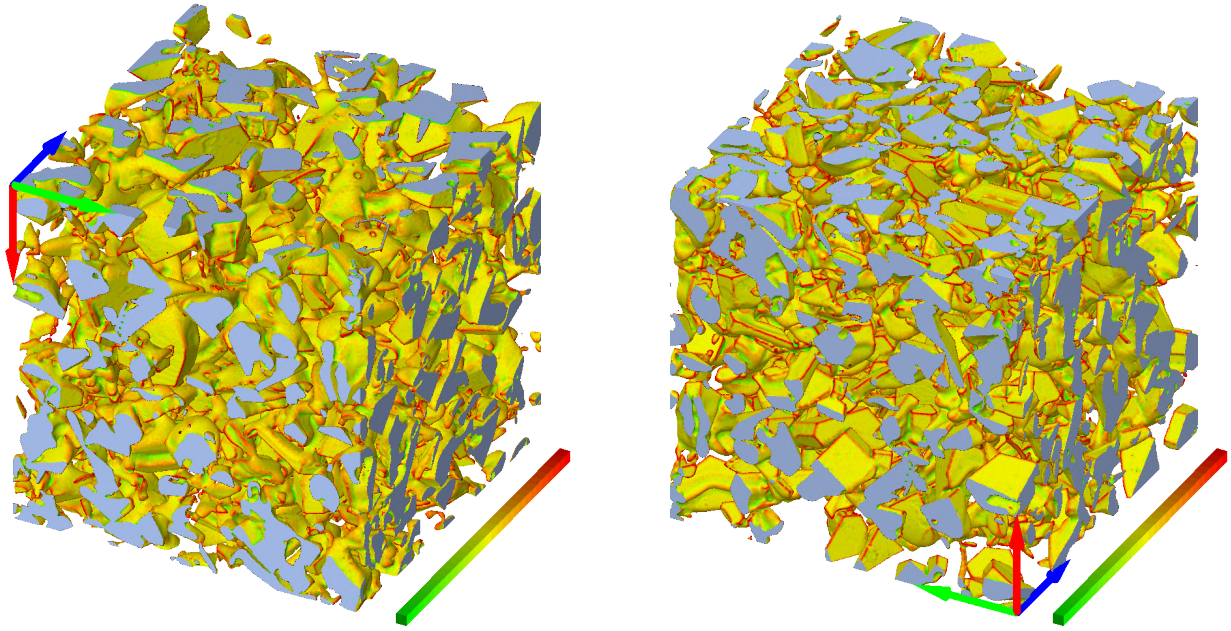

Figure S51. Downward (left) and upward (right) views of the whole image volume, where the mean local curvature is represented in each point of the surface. Concave surfaces are shown in green, convex surfaces in red, and flat surfaces in yellow (see colorbars from -30 to +30 mm^{-1}). The side of each viewing cube amounts to 5.89 mm. The blue, green, and red arrows, correspond to the x, y, and z coordinate axes, respectively.

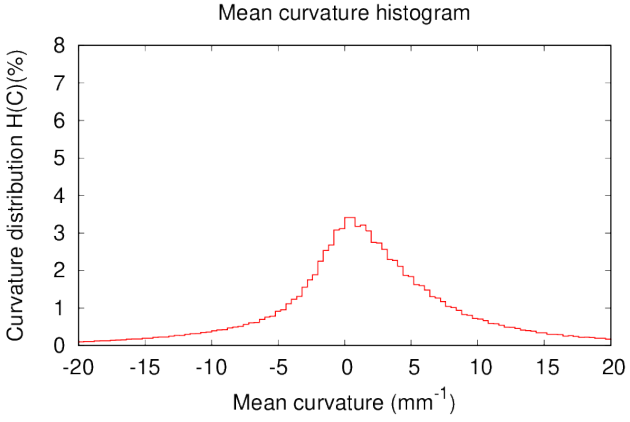

Figure S52. Mean curvature distribution on the whole image, from -20 to +20 mm^{-1}. Each bin is 0.4 mm^{-1} wide.

Image 0A

Table S29.

Snow type	Image size (voxel)	Pixel size (µm)	ρ (kg m^{-3})	SSA (m^2 kg^{-1})	d (mm)	$\overline{\mathrm{MC}}$ (mm^{-1})	IQR$_{\mathrm{MC}}$ (mm^{-1})
RG	700	8.392	314.83	27.68	0.2367	4.87	9.38

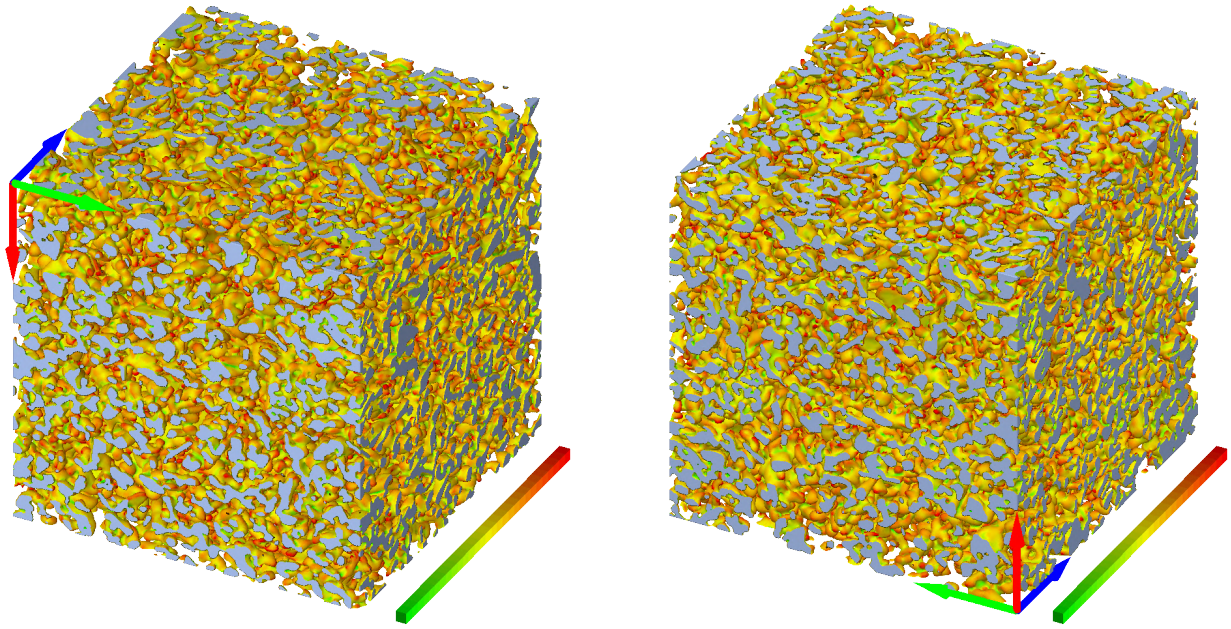

Figure S53. Downward (left) and upward (right) views of the whole image volume, where the mean local curvature is represented in each point of the surface. Concave surfaces are shown in green, convex surfaces in red, and flat surfaces in yellow (see colorbars from -30 to +30 mm^{-1}). The side of each viewing cube amounts to 5.87 mm. The blue, green, and red arrows, correspond to the x, y, and z coordinate axes, respectively.

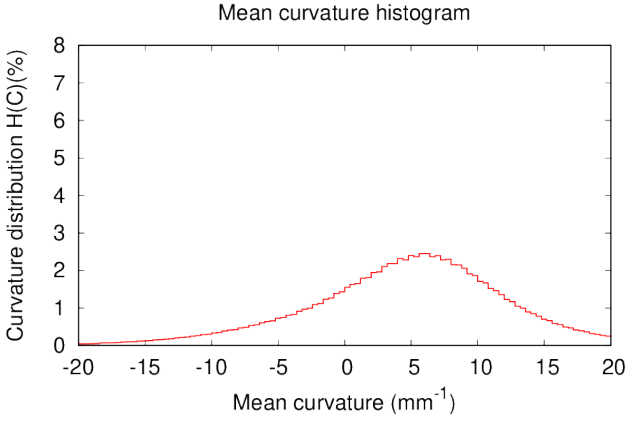

Figure S54. Mean curvature distribution on the whole image, from -20 to +20 mm^{-1}. Each bin is 0.4 mm^{-1} wide.

Image 1A

Table S30.

Snow type	Image size (voxel)	Pixel size (µm)	ρ (kg m^{-3})	SSA (m^2 kg^{-1})	d (mm)	$\overline{\mathrm{MC}}$ (mm^{-1})	IQR$_{\mathrm{MC}}$ (mm^{-1})
RG	700	8.395	275.04	23.37	0.2800	4.67	9.17

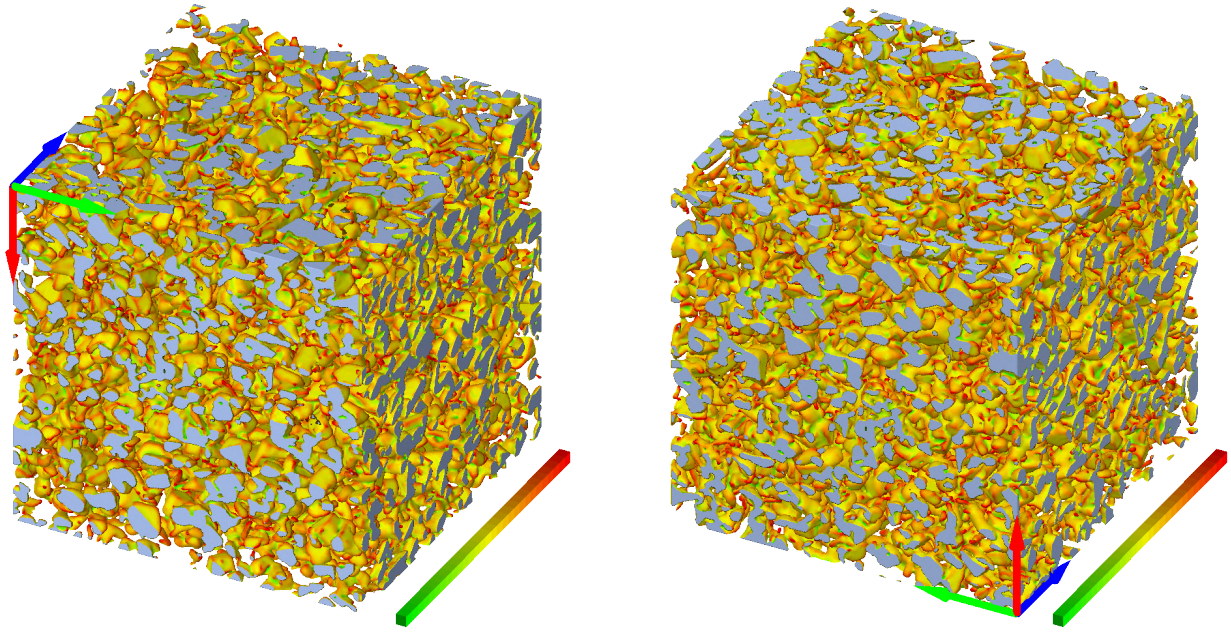

Figure S55. Downward (left) and upward (right) views of the whole image volume, where the mean local curvature is represented in each point of the surface. Concave surfaces are shown in green, convex surfaces in red, and flat surfaces in yellow (see colorbars from -30 to +30 mm^{-1}). The side of each viewing cube amounts to 5.88 mm. The blue, green, and red arrows, correspond to the x, y, and z coordinate axes, respectively.

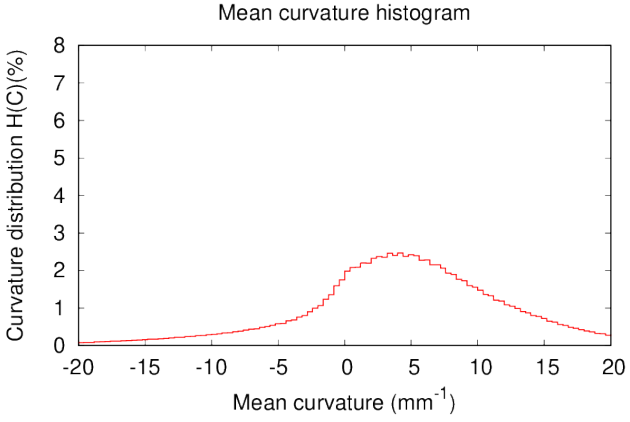

Figure S56. Mean curvature distribution on the whole image, from -20 to +20 mm^{-1}. Each bin is 0.4 mm^{-1} wide.

Image 2A

Table S31.

Snow type	Image size (voxel)	Pixel size (µm)	ρ (kg m^{-3})	SSA (m^2 kg^{-1})	d (mm)	$\overline{\mathrm{MC}}$ (mm^{-1})	IQR$_{\mathrm{MC}}$ (mm^{-1})
FC	700	8.373	282.70	20.75	0.3154	3.53	9.03

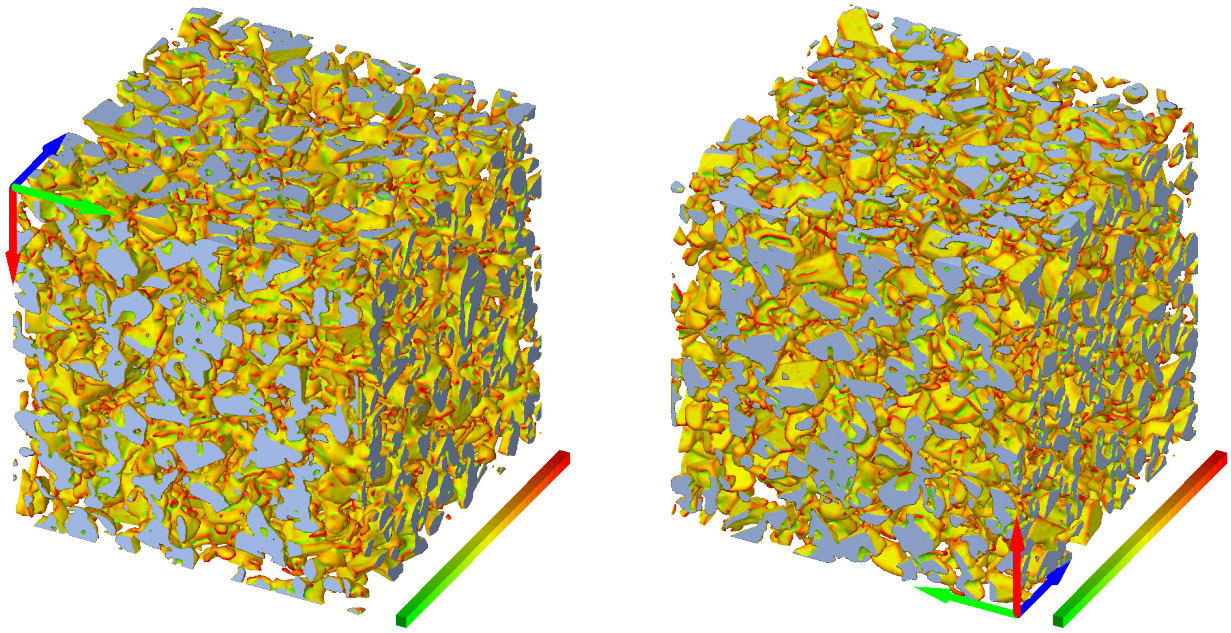

Figure S57. Downward (left) and upward (right) views of the whole image volume, where the mean local curvature is represented in each point of the surface. Concave surfaces are shown in green, convex surfaces in red, and flat surfaces in yellow (see colorbars from -30 to +30 mm^{-1}). The side of each viewing cube amounts to 5.86 mm. The blue, green, and red arrows, correspond to the x, y, and z coordinate axes, respectively.

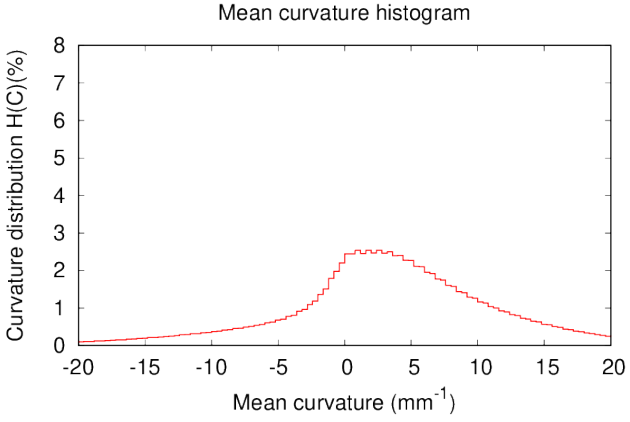

Figure S58. Mean curvature distribution on the whole image, from -20 to +20 mm^{-1}. Each bin is 0.4 mm^{-1} wide.

Image 3A

Table S32.

Snow type	Image size (voxel)	Pixel size (µm)	ρ (kg m^{-3})	SSA (m^2 kg^{-1})	d (mm)	$\overline{\mathrm{MC}}$ (mm^{-1})	IQR$_{\mathrm{MC}}$ (mm^{-1})
DH	700	8.400	274.79	18.18	0.3600	2.65	8.52

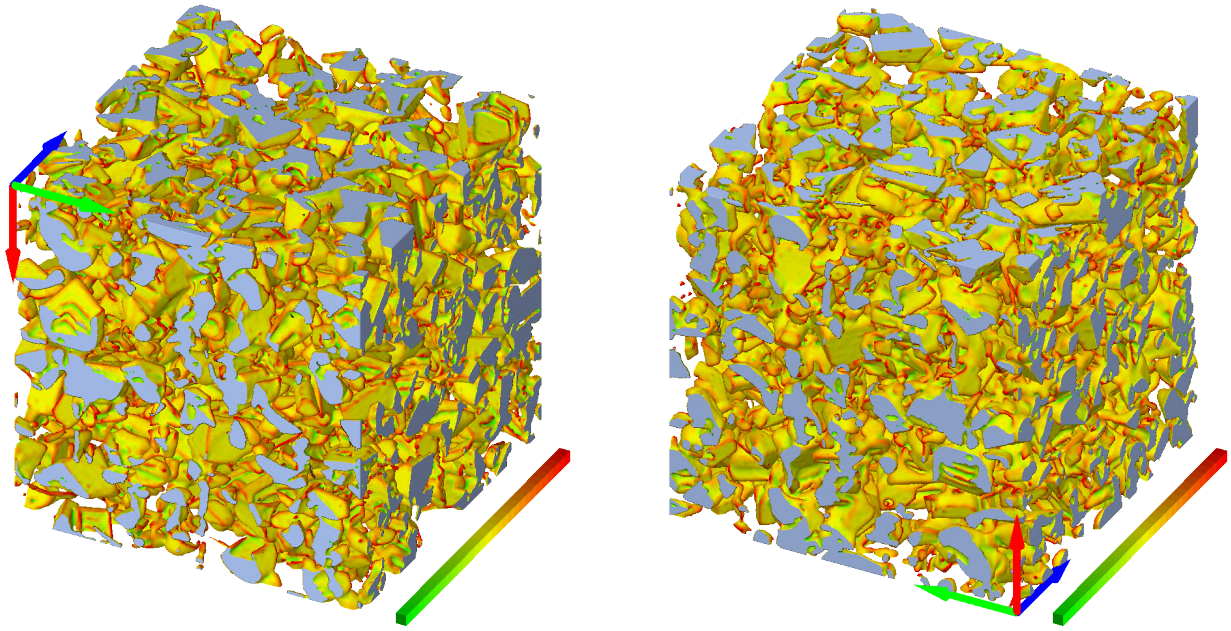

Figure S59. Downward (left) and upward (right) views of the whole image volume, where the mean local curvature is represented in each point of the surface. Concave surfaces are shown in green, convex surfaces in red, and flat surfaces in yellow (see colorbars from -30 to +30 mm^{-1}). The side of each viewing cube amounts to 5.88 mm. The blue, green, and red arrows, correspond to the x, y, and z coordinate axes, respectively.

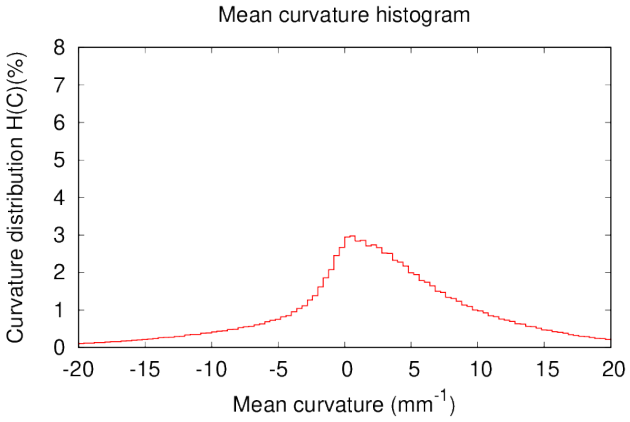

Figure S60. Mean curvature distribution on the whole image, from -20 to +20 mm^{-1}. Each bin is 0.4 mm^{-1} wide.

Image 4A

Table S33.

Snow type	Image size (voxel)	Pixel size (µm)	ρ (kg m^{-3})	SSA (m^2 kg^{-1})	d (mm)	$\overline{\mathrm{MC}}$ (mm^{-1})	IQR$_{\mathrm{MC}}$ (mm^{-1})
DH	700	8.397	315.31	15.19	0.4309	1.34	7.61

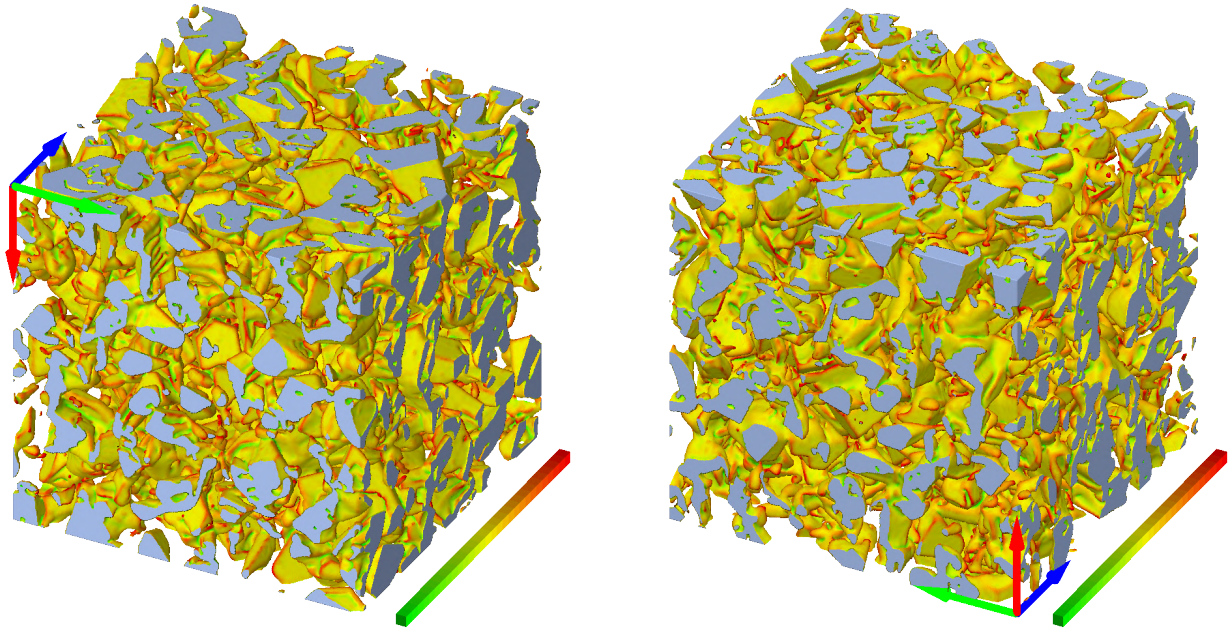

Figure S61. Downward (left) and upward (right) views of the whole image volume, where the mean local curvature is represented in each point of the surface. Concave surfaces are shown in green, convex surfaces in red, and flat surfaces in yellow (see colorbars from -30 to +30 mm^{-1}). The side of each viewing cube amounts to 5.88 mm. The blue, green, and red arrows, correspond to the x, y, and z coordinate axes, respectively.

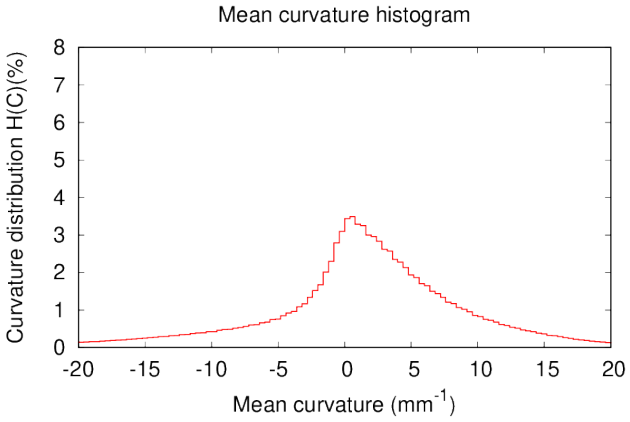

Figure S62. Mean curvature distribution on the whole image, from -20 to +20 mm^{-1}. Each bin is 0.4 mm^{-1} wide.

Image 5A

Table S34.

Snow type	Image size (voxel)	Pixel size (µm)	ρ (kg m^{-3})	SSA (m^2 kg^{-1})	d (mm)	$\overline{\mathrm{MC}}$ (mm^{-1})	IQR$_{\mathrm{MC}}$ (mm^{-1})
DH	1000	9.655	286.12	14.89	0.4395	1.65	7.75

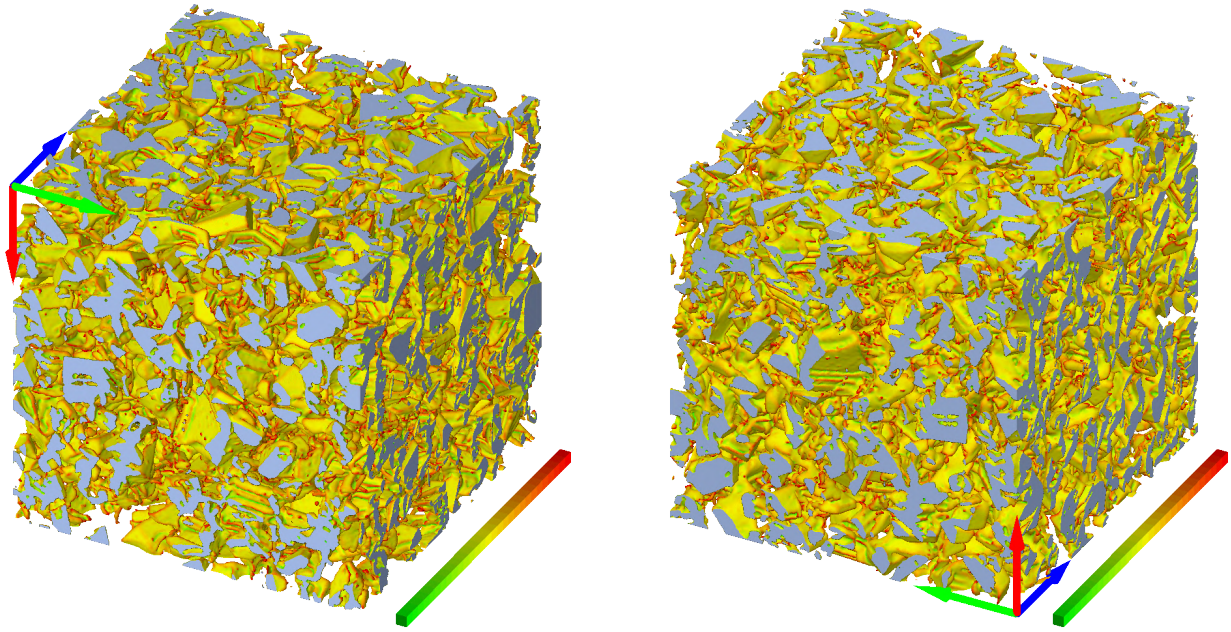

Figure S63. Downward (left) and upward (right) views of the whole image volume, where the mean local curvature is represented in each point of the surface. Concave surfaces are shown in green, convex surfaces in red, and flat surfaces in yellow (see colorbars from -30 to +30 mm^{-1}). The side of each viewing cube amounts to 9.66 mm. The blue, green, and red arrows, correspond to the x, y, and z coordinate axes, respectively.

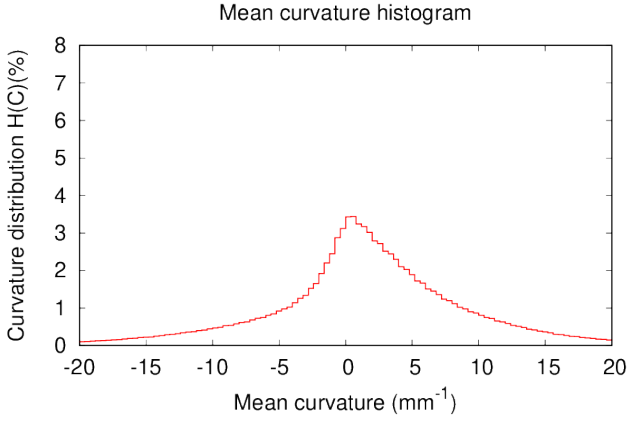

Figure S64. Mean curvature distribution on the whole image, from -20 to +20 mm^{-1}. Each bin is 0.4 mm^{-1} wide.

Image 7A

Table S35.

Snow type	Image size (voxel)	Pixel size (µm)	ρ (kg m^{-3})	SSA (m^2 kg^{-1})	d (mm)	$\overline{\mathrm{MC}}$ (mm^{-1})	IQR$_{\mathrm{MC}}$ (mm^{-1})
DH	950	9.672	309.95	13.42	0.4882	1.05	7.87

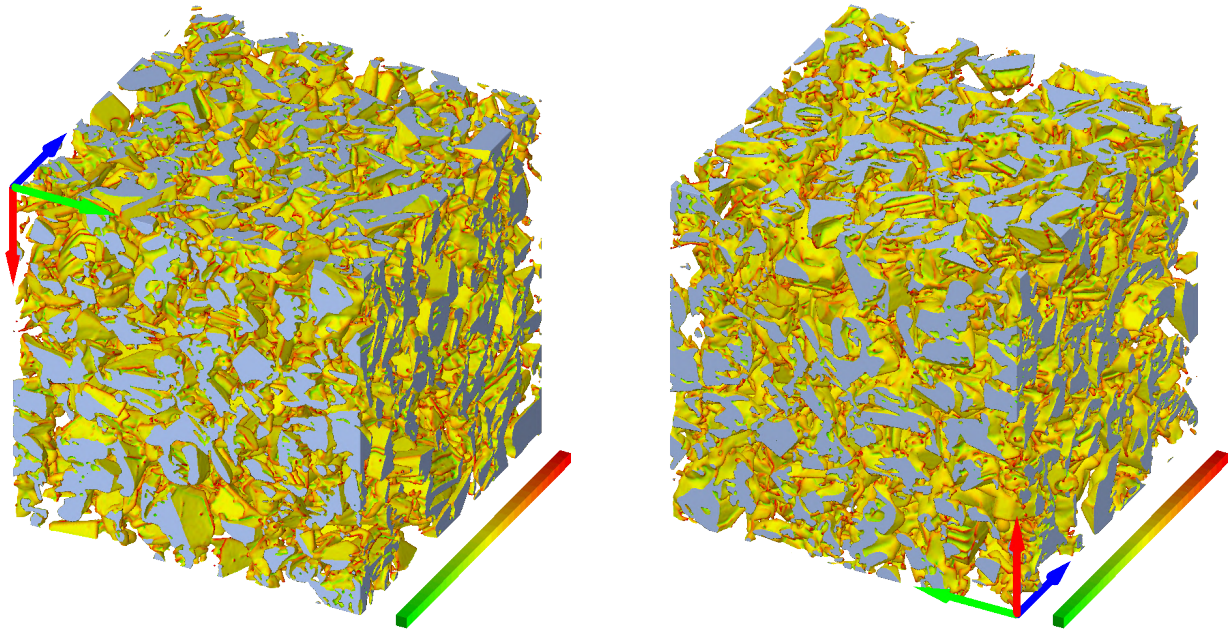

Figure S65. Downward (left) and upward (right) views of the whole image volume, where the mean local curvature is represented in each point of the surface. Concave surfaces are shown in green, convex surfaces in red, and flat surfaces in yellow (see colorbars from -30 to +30 mm^{-1}). The side of each viewing cube amounts to 9.19 mm. The blue, green, and red arrows, correspond to the x, y, and z coordinate axes, respectively.

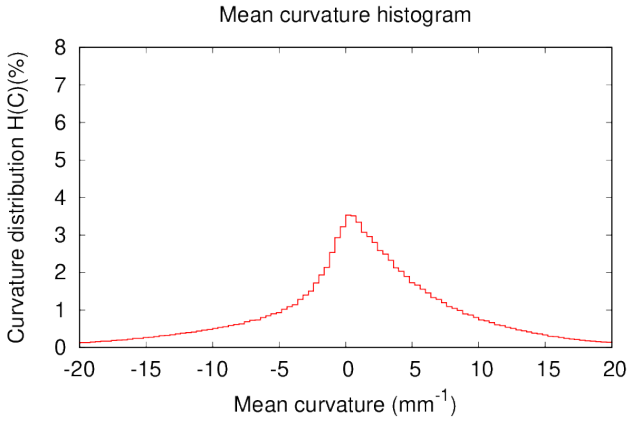

Figure S66. Mean curvature distribution on the whole image, from -20 to +20 mm^{-1}. Each bin is 0.4 mm^{-1} wide.

Image grad3

Table S36.

Snow type	Image size (voxel)	Pixel size (µm)	ρ (kg m^{-3})	SSA (m^2 kg^{-1})	d (mm)	$\overline{\mathrm{MC}}$ (mm^{-1})	IQR$_{\mathrm{MC}}$ (mm^{-1})
DH	600	10.000	369.20	21.84	0.2996	0.76	11.32

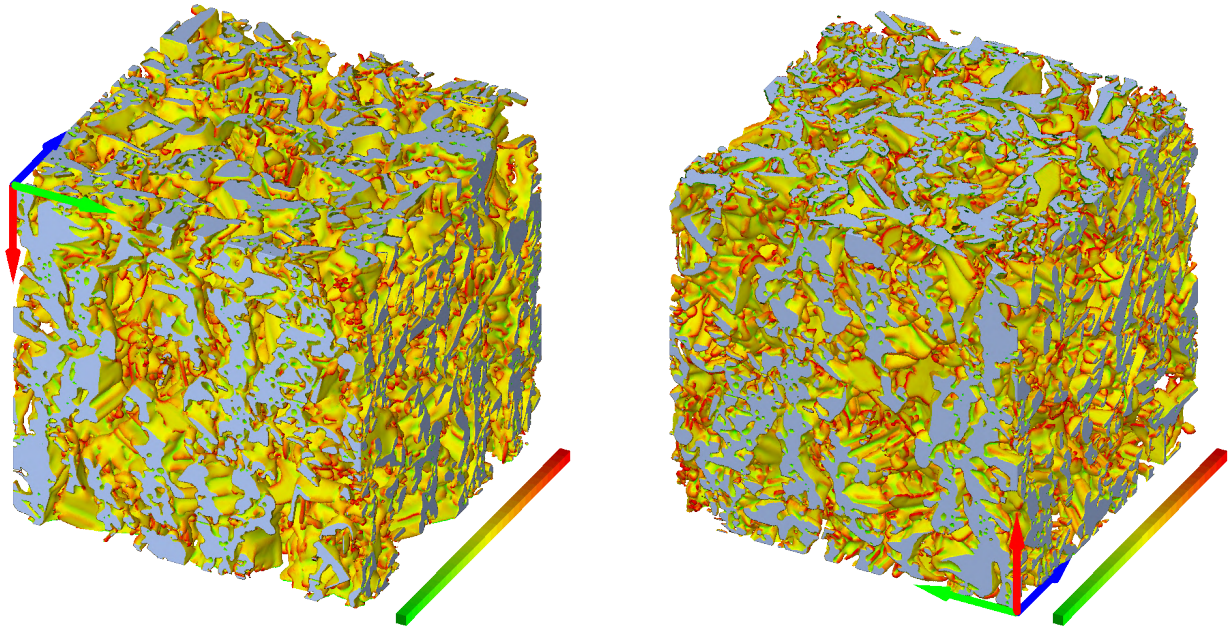

Figure S67. Downward (left) and upward (right) views of the whole image volume, where the mean local curvature is represented in each point of the surface. Concave surfaces are shown in green, convex surfaces in red, and flat surfaces in yellow (see colorbars from -30 to +30 mm^{-1}). The side of each viewing cube amounts to 6.00 mm. The blue, green, and red arrows, correspond to the x, y, and z coordinate axes, respectively.

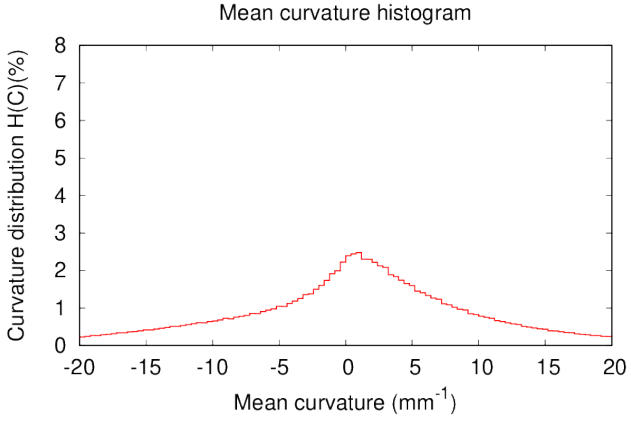

Figure S68. Mean curvature distribution on the whole image, from -20 to +20 mm^{-1}. Each bin is 0.4 mm^{-1} wide.

References

Calonne, N., Flin, F., Morin, S., Lesaffre, B., Rolland du Roscoat, S., and Geindreau, C.: Numerical and experimental investigations of the effective thermal conductivity of snow, Geophys. Res. Lett., 38, L23 501, https://doi.org/10.1029/2011GL049234, 2011.

Calonne, N., Flin, F., Geindreau, C., Lesaffre, B., and Rolland du Roscoat, S.: Study of a temperature gradient metamorphism of snow from 3-D images: time evolution of microstructures, physical properties and their associated anisotropy, The Cryosphere, 8, 2255–2274, https://doi.org/10.5194/tc-8-2255-2014, 2014.

Coléou, C., Lesaffre, B., Brzoska, J.-B., Ludwig, W., and Boller, E.: Three-dimensional snow images by X-ray microtomography, Annals of Glaciology, 32, 75–81, https://doi.org/10.3189/172756401781819418, 2001.

Fierz, C., Armstrong, R. L., Durand, Y., Etchevers, P., Greene, E., McClung, D. M., Nishimura, K., Satyawali, P. K., and Sokratov, S. A.: The international classification for seasonal snow on the ground, IHP-VII Technical Documents in Hydrology, IACS Contribution n° 1, 83, https://unesdoc.unesco.org/ark:/48223/pf0000186462, 2009.

Flin, F. and Brzoska, J.-B.: The temperature gradient metamorphism of snow: vapour diffusion model and application to tomographic images, Ann. Glaciol., 49, 17–21, https://doi.org/10.3189/172756408787814834, 2008.

Flin, F., Brzoska, J.-B., Lesaffre, B., Coléou, C., and Pieritz, R. A.: Three-dimensional geometric measurements of snow microstructural evolution under isothermal conditions, Annals of Glaciology, 38, 39–44, https://doi.org/10.3189/172756404781814942, 2004.

Flin, F., Lesaffre, B., Dufour, A., Gillibert, L., Hasan, A., Rolland du Roscoat, S., Cabanes, S., and Puglièse, P.: On the computations of specific surface area and specific grain contact area from snow 3D images, in: Physics and Chemistry of Ice, edited by Y. Furukawa, pp. 321–328, Hokkaido University Press, Sapporo, Japan, https://frederic-flin.github.io/pdf/flin_2011_ssa_sgca.pdf, 2011.